REPUBLIC OF TÜRKİYE

ALTINBAŞ UNIVERSITY

Institute of Graduate Studies

Electrical and Computer Engineering

# NEURAL NETWORK TRAINING METHOD FOR CLASSIFICATIONS OF DIABETIC RETINOPATHY IMAGE DATA ON MATLAB

**Ahmed Afeef Ameen SALIH**

Master's Thesis

Supervisor

Asst. Prof. Dr. Ayça KURNAZ TÜRKBEN

Istanbul, 2023

# NEURAL NETWORK TRAINING METHOD FOR CLASSIFICATIONS OF DIABETIC RETINOPATHY IMAGE DATA ON MATLAB

**Ahmed Afeef Ameen SALIH**

Electrical and Computer Engineering

Master's Thesis

ALTINBAŞ UNIVERSITY

2023

The thesis/dissertation titled NEURAL NETWORK TRAINING METHOD FOR CLASSIFICATIONS OF DIABETIC RETINOPATHY IMAGE DATA ON MATLAB prepared by Ahmed SALIH and submitted on 13/04/2023 has been **accepted unanimously** for the degree of Master of Arts/Master of Science in Electrical and Computer Engineering.

Dr. Öğr. Üye. Ayça KURNAZ TÜRKBEN

Thesis Defense Committee Members:

| | | |
|---|---|---|
| Academic Title - First/Last Name | Department, University | _____ |
| Academic Title - First/Last Name | Department, University | _____ |
| Academic Title - First/Last Name | Department, University | _____ |
| Academic Title - First/Last Name | Department, University | _____ |
| Academic Title - First/Last Name | Department, University | _____ |

I hereby declare that this thesis/dissertation meets all format and submission requirements of a Electrical and Computer Engineering Master's thesis.

Submission date of the thesis to the Graduate Education Institute: 13/04/2023

I hereby declare that all information presented in this graduation project has been obtained in full accordance with academic rules and ethical conduct. I also declare all unoriginal materials and conclusions have been cited in the text and all references mentioned in the Reference List have been cited in the text, and vice versa as required by the abovementioned rules and conduct.

Ahmed Afeef Ameen SALIH

Signature

# ABSTRACT

## NEURAL NETWORK TRAINING METHOD FOR CLASSIFICATIONS OF DIABETIC RETINOPATHY IMAGE DATA ON MATLAB

SALIH, Ahmed Afeef

M.Sc, Electrical and Computer Engineering, Altınbaş University,

Supervisor: Asst. Prof. Dr. Ayça Kurnaz TÜRKBEN

Date: April / 2023

Pages: 64

Deep learning was used in this research to develop a method that could identify hard exudates in DR fundus pictures. Patients with diabetic retinopathy need to be able to differentiate between hard exudates and other symptoms of sickness. This innovative technique accurately identifies hard exudates 99.7% of the time. In the future, detection will also include blood flow and microaneurysms in addition to soft exudates. In addition to this, we need to quantify DR by utilizing segmented pictures. There are two approaches that improve model precision. Then, change the dimensions of the picture patch. The next thing that we could do is investigate the role that picture patches have in the accuracy of the forecast. Convolutional neural networks are utilized in the second technique, which performs an analysis on the first and last 16 unpredicted pixels in each row and column.

**Keywords:** Convolutional Neural Network, Deep Learning, Image Processing, Hard Exudates, Retinopathy Diabetes, SGD.

# TABLE OF CONTENTS

**Pages**

# LIST OF TABLES

**Pages**

# LIST OF FIGURES

**Pages**

# ABBREVIATIONS

| | | |
|---|---|---|
| TDMA | : | Time Division Multiple Access |
| OFDM | : | Orthogonal Frequency Division Multiplexing |
| PAN | : | Personal Area Network |
| IoT | : | Internet of Things |
| FSK | : | Frequency Shift Keying |
| DR | : | Diabetic Retinopathy |
| AI | : | Artificial Intelligence |

# 1. INTRODUCTION

## 1.1 INTRODUCTION

Diabetic retinopathy (DR), an eye disease that can cause whole or partial blindness. A survey by the International Diabetes Federation estimates that by 2045, almost 6 billion individuals throughout the world would have diabetes. Some researchers have suggested that DR is the most dangerous condition to human eyes. Therefore, it is essential that people with DR receive prompt diagnosis and treatment to prevent blindness. Blindness from DR can be reduced to 5% if patients are diagnosed and treated promptly, as is generally agreed upon [1]. For over 50 years, the World Health Organization (WHO) has disseminated broad standards for identifying and classifying diabetes. Developed as a reference for diagnosing and categorizing diabetes and its complications, the final edition was published in 1998. The World Health Organization convened a conference in Geneva with the technical advisory group of the International Diabetes Federation (IDF) to review and modify the present WHO recommendations [2]. According to the 2013 estimate from the International Diabetes Federation, almost 385 million people worldwide have diabetes, the vast majority of them have type-2 diabetes. As of 2035, experts estimate that the appropriate sum will reach $592,000,000 [3]. According to the World Health Organization, diabetes is the fourth greatest cause of mortality, and it results in enormous monetary, social, and healthcare costs. Amazingly, diabetes-related cardiovascular issues both large and little drastically reduce both life expectancy and quality of life [4]. Thus, the definition and categorization of diabetes are major research concerns, and many researchers have been hard at work trying to come up with new solutions.

Diabetic retinopathy is a leading cause of permanent vision loss in diabetics. Diabetic retinopathy, to sum up, is a potentially blinding eye disease caused by long-term diabetes mellitus. As a consequence, blindness is a common complication, particularly in developed countries. Now more than ever, early diagnosis and treatment of diabetic retinopathy are crucial for preventing people from getting the condition that ultimately leads to blindness or, at the very least, stopping the progression of the disease. Consequently, it is extremely desirable to test all diabetes patients. While automated grading may be inaccurate at times, manual grading always yields accurate results since it requires so much experience.

Computerized scanning approaches based on colored fundus images have seen extensive development throughout time [5, 6]. Even with the advent of digital fundus imaging, it is still difficult to diagnose diabetic retinopathy, prompting the development of new treatments. Intelligent diagnosis systems are the natural progression from imaging and computer vision-based diagnostic tools. Background.

High blood sugar causes hyperglycemia, which in turn damages retinal pericytes. [7]. Diabetic retinopathy (DR) is the medical name for the damage done to the retina by diabetes. It's a vascular condition of the retina that may cause vision loss. Capillary regression and angiogenesis are two examples of how DR affects vascular networks. Patients with diabetes mellitus often have retinal abnormalities known as diabetic retinopathy (DR). High blood sugar levels are the root cause of the metabolic disease known as diabetes mellitus (DM). Most people with DR don't show any symptoms until the condition is already advanced. As diabetics are now living longer than ever before, there has been a rise in the frequency of diabetic retinopathy, a main cause of blindness. Those who have diabetes are more likely to suffer from this illness, which may cause irreversible vision loss. Retinal blood vessels are compromised. Moreover, it causes extensive damage to the retina's blood vessels. As a consequence of diabetes, blood vessels may form in the eye's drainage angle. This may lead to a rise in eye pressure, which can induce glaucoma. Because of this, harm is done to the visual nerve. [8]. The visual differences between normal and diabetic eyes are shown in Figure 1.1.

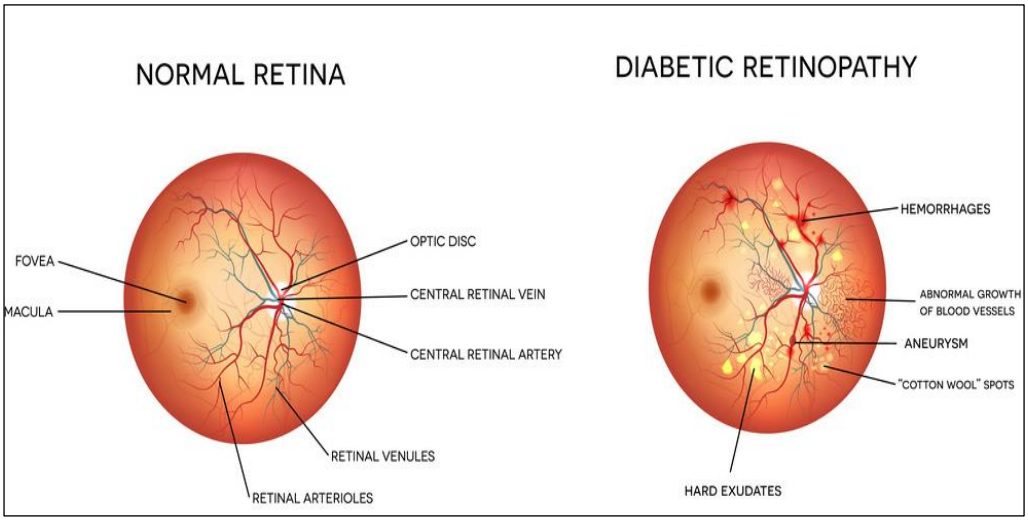


**Figure 1.1:** Comparison Between Diabetics and Healthy Eyes [7].

A disease called as moderate non-proliferative diabetic retinopathy occurs when fatty deposits begin to form at the retina's fragile end due to diabetes. A maculopathy caused by diabetic exudates is called diabetic maculopathy. When the microinfarcts in the retina restrict the blood vessels, the condition is called "retinopathy," and it worsens with time. These little infarcts are called soft exudates in the medical field. All three of these anomalies must be present for a diagnosis of severe non-proliferative diabetic retinopathy to be established [9].

First, it causes occlusion, and then, very fast, visual loss. The disease's early stages are characterized by a lack of obvious symptoms. Retinal microaneurysms are enlarged blood vessels that are a feature of this disorder. Negligence increases the eye's condition, which causes more severe spots to form and damages to the retinal vessels, which ultimately causes complete blindness. Reducing the likelihood of blindness in those at high risk may be as simple as identifying DR early and keeping an eye on them. The complex image produced by color fundus photography makes it difficult and error-prone for humans to detect and classify diabetic retinopathy. Depending on their degree of severity, vascular lesions may be classified as either nonhyperplasia or hyperplasia [10]. Nonhyperplasia, the first stage of diabetic retinopathy (DR), may manifest as asymptomatic, mild, moderate, or severe disease. Patients do not experience any symptoms until the illness has progressed to a critical stage, by which time it is too late to effectively treat. Consequently, early identification and management are necessary to prevent vision loss or blindness as a result of diabetes. In other words, the condition may be detected, treated, and prevented if screenings are performed regularly. Moreover, it may slow the development of the condition. Screening methods that have traditionally been used, in which ophthalmologists manually evaluate and screen

images of the retina, fall well short of what is required [11]. Figure 1.2 depicts several theoretical frameworks and ongoing research projects that are mentioned in this study.

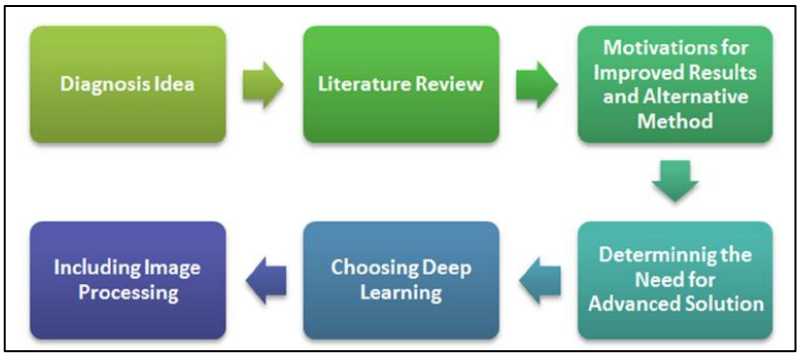


**Figure 1.2:** Ideas and Research Efforts on the Background of This Study [11].

In their search for DR, researchers have used a wide range of approaches, including learning-based, feature-based, classification-based, and other procedures. Deep learning is finding increasing utility in a wide variety of technical contexts, including semantic comprehension and picture recognition. However, the accuracy provided by feature extraction techniques and machine learning algorithms for classifying DR severity levels is insufficient. Since the introduction of deep learning (DL) methods, computer vision has achieved previously unthinkable precision [7]. Utilizing deep learning architecture, segmented fundus pictures may be classified as "Normal" or "Abnormal," meaning healthy or diabetic retinopathy damaged. Different approaches exist that use segmented pictures and the CNN to acquire knowledge from retinal scans. The extraction of the blood vasculature is accomplished via a method for identifying maximum principal curvatures. Morphological opening and adaptive histogram equalization are used to enhance and eliminate poorly segmented parts. To further boost the classifier's efficiency, a CNN model with two-way classification was developed. Classification is accomplished using a process that combines the squeezing, excitation, and bottleneck layers. The alternate structure has both convolution and pooling layers. Separate and distinct architectures in the modules provide trustworthy feature extraction. A test picture may be fed into both networks, and the result of the classification will be approved only if there is a consensus. Thus, the model outperforms its predecessors by a wide margin. [12]

## 1.2 PROBLEM STATEMENT

Retinal ischemia, macular edema, retinal permeability, and retinal neovascularization are all progressive diseases brought on by DR's underlying microvascular alterations. Without treatment, patients with DR might lose their eyesight permanently. Early diabetic retinopathy is characterized by microaneurysms and exudation, however it may be difficult to identify these symptoms. DR is the leading cause of blindness in people of working age in wealthy countries, with consequential economic effects, especially on healthcare systems. Diagnosing, classifying, and staging the severity of DR allows for the most effective medication to be delivered, potentially preventing more than 90% of cases of vision loss with careful management of DR patients. Diabetes treatment requires input from a wide range of medical experts, making effective two-way communication between specialists in different domains essential. To better serve their patients, retina specialists, general ophthalmologists, internal medicine physicians, and endocrinologists must all acquire a common lexicon. Retinal capillaries are compromised by high blood sugar levels. Microaneurysms, or protrusions of the vessel lumens, develop as a consequence of the increased fragility of the capillary walls. Figure 1.3 demonstrates the consequences of a burst microaneurysm on the retina. Microaneurysms (A) and their larger counterparts (B) (Figure 1.3).

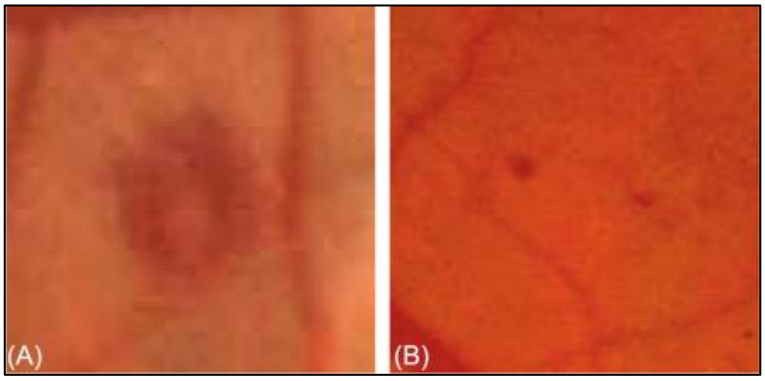


**Figure 1.3:** (A) Large Microaneurysm with Central Reflex and (B) Microaneurysms [10].

The knowledge may be utilized to ascertain if the retina is in the proliferative or nonproliferative DR stage. Segmenting the fundus picture into regions with exudates, microaneurysms, optical disks, or hemorrhages is important. To follow is a breakdown of the system's highest priorities. Image quality is improved when scaling is performed in the

preprocessing stage. To improve the accuracy of recognizing MAs, exudates, hemorrhages, and optical discs, an image segmentation approach is required. Most urgent issues include:

a. When compared to low-resolution photos, high-resolution photographs performed better. Developing the model took a lot of time and energy, but it paid off in the end. But the model's performance suffered when photographed in poor quality.

b. Images containing noise and a wide variety of distributions may impact the model's accuracy and efficiency, which raises concerns about data quality.

c. One technique could not be used universally when attempting to categorize images across many different datasets and many different computer vision and image classification applications.

## 1.3 AIM AND OBJECTIVES

The purpose of this study was to develop algorithms for the automatic detection of DR in people with diabetes mellitus using photographs of their retinal fundi. Research aims at this point are to:

a. Help doctors see the first signs of diabetic retinopathy so they can treat it.

b. Less essential aspects that contribute to the sickness should be ignored during training in order to lighten the load on the classifiers.

c. Use high-resolution images to aid in diagnosis.

## 1.4 OUTLINE OF THE THESIS

This study explores techniques in Diabetic retinopathy severity ratings. Features extracted, images pre-processed, and a model trained to generate the suggested procedure. Hereafter, this thesis will be divided into the following 5 chapters. Initial Chapter: System Overview and Context Diabetic retinopathy grading and deep learning in medical images are discussed in Chapter 2. The third chapter provides an overview of related literature. Our experimental

procedure, data analysis, and interpretation are all detailed in Chapter 4. Experiments are summarized and discussed in Chapter 5.

# 2. LITERATURE REVIEW

## 2.1 INTRODUCTION

Diabetic retinopathy and its many phases, as well as its aetiology and diagnostic and grading criteria, will be discussed in this chapter. Considering its relevance to AI and neural network categorization, and briefly examine some recent research in those fields below.

## 2.2 DIABETES

According to the World Diabetes Federation, in 2015 there were 415 million people aged 20-79 who were diagnosed with diabetes mellitus (IDF). By 2040, this number is projected to rise by another 200 million, making diabetes a major public health problem all across the globe. [13] When a person has diabetes, they constantly struggle with high blood sugar levels, which may negatively impact their health and happiness for the rest of their lives. It's the second leading cause of death worldwide and a major contributor to illness and disability. Diabetes mellitus has two primary causes: an inherited or acquired chronic pancreatic insufficiency in making insulin or an ineffectiveness of the insulin produced. Millions of people all around the globe are affected by this silent killer. Non-hypoglycemic and severe metabolic disorders not connected to diabetes are examined in depth, along with their causes, classifications, incidences, preventative measures, and treatments, in this research [14]. To determine the current burden of GDM, we performed a PubMed literature search and cross-referenced pertinent references of eligible publications on GDM prevalence from 2005 to 2018. From the list of relevant studies that met the criteria of the search WHO statistics shown in figure 2.1. [15]

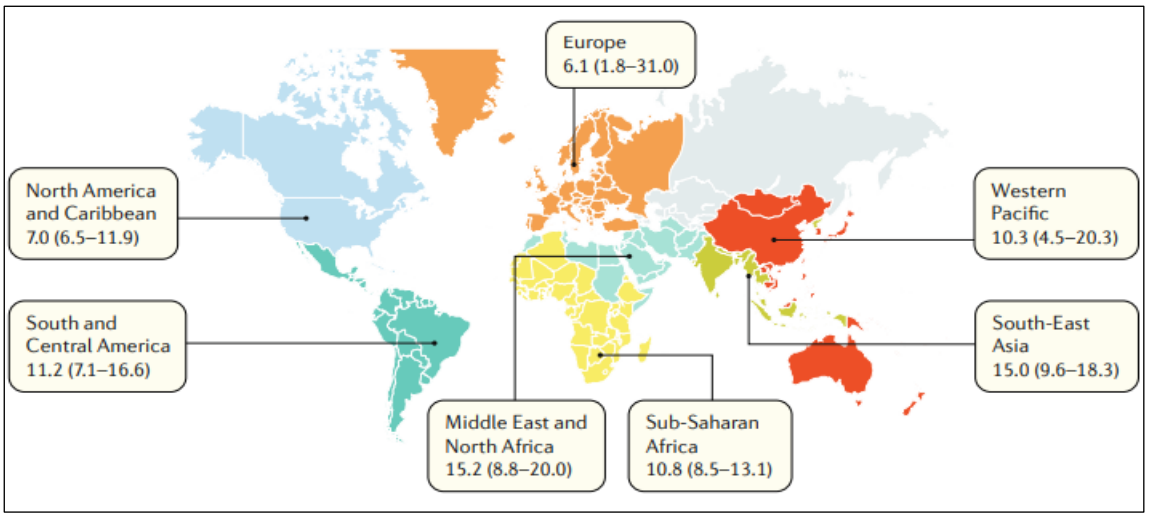


**Figure 2.1:** Gestational Diabetes Mellitus (GDM) Interquartile Range Prevalence (%) by WHO [15].

### 2.2.1 Diabetes Aetiology

Type 1 DM, type 2 DM, and gestational DM are the three main subtypes of DM based on their etiologies and clinical presentations (GDM). There are a few more, less common types of diabetes, including monogenic diabetes and secondary diabetes. [16][17][18][19]

a. Type 1 Diabetes Mellitus (T1DM)

Five to ten percent of all instances of diabetes are attributable to type 1 diabetes mellitus (T1DM), which is caused by the autoimmune death of insulin-producing beta cells in the pancreatic islets. Although though Type 1 Diabetes may affect anybody at any time, it often manifests in young adults.

b. Type 2 Diabetes Mellitus

Almost 90% of all occurrences of diabetes mellitus are of the type 2 kind (T2DM). Type 2 diabetes is characterized by insulin resistance, an impaired response to insulin. As insulin loses its efficacy, the body produces more of the hormone in an initial attempt to keep glucose levels stable; however, this compensatory increase in insulin production eventually waneseventually leading to type 2 diabetes. People over the age of 45 are at increased risk for developing type 2 diabetes. However, as the prevalence of overweight individuals, unhealthy lifestyles, and high-calorie meals rises, the disease is increasingly seen in younger age groups.

c. Gestational Diabetes Mellitus

When hyperglycaemia is initially identified when a woman is pregnant, it is called gestational diabetes mellitus (GDM). Women who are pregnant often suffer from GDM in their third trimester. The American Diabetes Association (ADA) reports that 7% of all pregnancies are affected with GDM. Future development of type 2 diabetes mellitus is more likely in women with GDM and their offspring. Complications including as hypertension, preeclampsia, and hydramnios may make GDM more severe and increase the need for surgical therapies. Those who are older, overweight, put on too much weight during pregnancy, had children with birth abnormalities or died before they were born, or had a close relative with diabetes are at a higher risk of developing GDM.

d. Monogenic Diabetes

This kind of diabetes results from a change in a single autosomal dominant gene. Neonatal diabetes mellitus and maturity-onset diabetes in children are two examples of monogenic forms of diabetes (MODY). "Monogenic diabetes" accounts for 1-5% of all cases of diabetes. Presenting symptoms of MODY, a genetic condition, often emerge in young individuals under the age of 25.

e. Secondary Diabetes

When the pancreas is affected by anything other than diabetes, the result is called secondary diabetes. [20]

### 2.2.2 Risk Factors of Diabetic

a. Obesity or being overweight (body mass index (BMI) 25kgm-2)

b. Advanced age

c. Ancestry other than white

d. Type 2 diabetes mellitus in the family

e. Fetal male

f. Genetic factors

g. Ovarian polycystic syndrome

h. Smoking cigarettes

i. Psychosocial aspects (for example, depression in pregnancy)

j. Leading a sedentary lifestyle both before and during pregnancy [21]

## 2.3 RETHINOPATHY DIABETIC DISEASE

A staggering 30 percent of diabetics will develop diabetic retinopathy [22]. It accounts for half of all cases of blindness in those aged 24 to 70 [23]. Type 1 diabetics seem to have a higher DR prevalence than type 2 diabetics [24]. Between 25% and 80% of those with T1D will acquire DR after 15 years. [25]. Most persons with DR have no idea they have it until the disease has progressed enough. Although diabetics are now living longer than ever before, the incidence of diabetic retinopathy, a major cause of blindness, has increased. Those who have diabetes are more likely to suffer from this illness, which may cause irreversible vision loss. Retinal blood vessels are compromised. Moreover, it causes extensive damage to the retina's blood vessels. As a consequence of diabetes, blood vessels may form in the eye's drainage angle. This may lead to a rise in ocular pressure, which can induce glaucoma. Because of this, harm is done to the visual nerve. [26] Figure 2.2 shows a simplified diagram of the many factors that might affect a disease's progression.

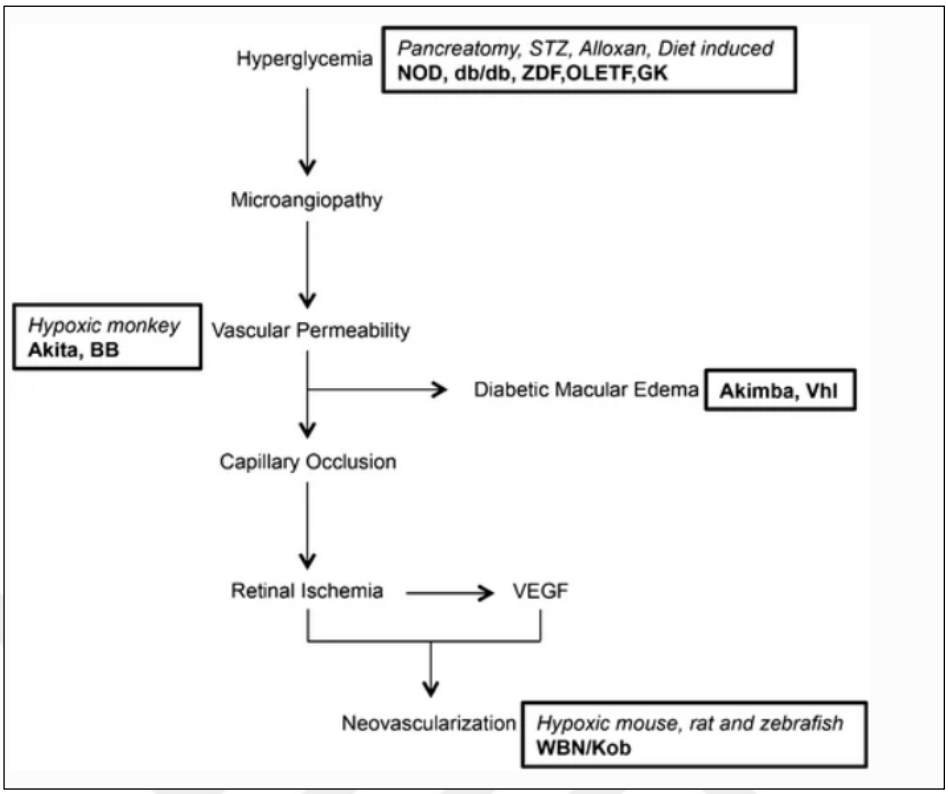


**Figure 2.2:** Schematic Representation of Diabetic Retinopathy (DR) Disease Progression [26].

Inflammation of the blood vessels, known as microangiopathy, is brought on by hyperglycaemia and hence initiates DR. This leads to vascular permeability, which in turn leads to diabetic macular edema and eventually, capillary occlusion. In the event of retinal ischemia due to blocked capillaries, VEGF levels rise, leading to neovascularization. Isolated in boxes is the part of the route being studied by animal experiments. Genetic models are indicated by bold text, whereas induced models are shown by italics text. [27]

## 2.4 RETHINOPATHY DIAGNOSIS

Regular retinal screening is crucial for diabetic patients in order to identify and treat DR early on and reduce the risk of going blind [28]. Different types of lesions that present on a retinal scan can be used to identify DR. Microaneurysms (MA), haemorrhages (HM), and soft and hard exudates (EX) are examples of these lesions [29]. Due to the fragility of the vessel's walls, microaneurysms (MA), which manifest as tiny red circular dots on the retina, are the first indicator of DR. Sharp margins and a dimension of less than 125 m are present. According to Michael et al. [30], MA can be divided into six categories as seen in figure 2.3.

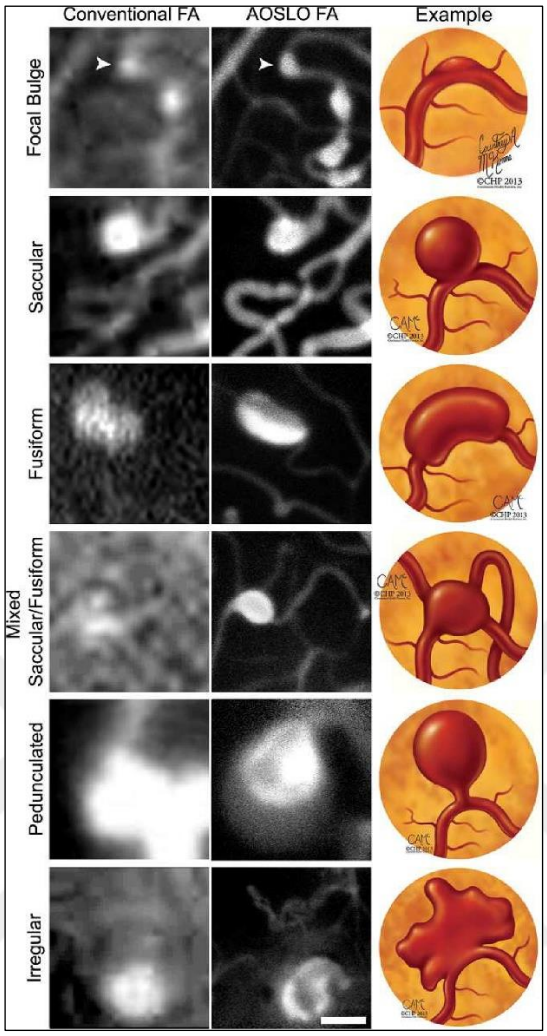


**Figure 2.3:** Types of MA [29].

Larger retinal patches may be seen when a haemorrhage is wider than 125 and has a wavy border. Figure 2.4 identifies two distinct forms of HM, which are referred to as "flame" (superficial HM) and "blot" (deeper HM). [31]

v 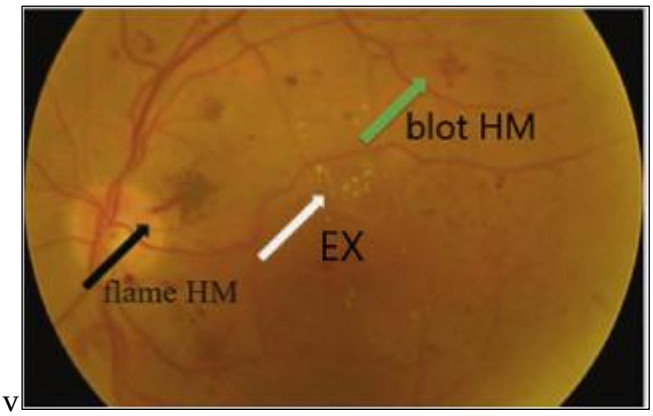


**Figure 2.4:** types of HM [30].

Red lesions are more likely to be MA or HM, whereas bright lesions are more likely to be exudates (both soft and hard) (EX). There are five phases of DR, depending on the presence or absence of certain lesions: levels of DR: none, mild, moderate, severe, and proliferative.

### 2.4.1 Diabetic Retinopathy Stages

a. No DR (normal):

At this stage, diabetic retinopathy has not yet caused any noticeable damage to the eye. Therefore, the eye seems to be in good condition.

b. MildDR:

The first stage of DR is characterized by swelling of the microscopic blood vessel sections, which causes damage to the visual nerve.

c. ModerateDR:

The second stage of DR, known as moderate DR or moderate non-proliferative retinopathy, results in some of the retina's blood veins becoming blocked.

d. SevereDR:

The third stage, also known as severe non proliferative retinopathy, is characterized by an even greater narrowing of the blood vessels. When blood flow is restricted, this has an effect on parts of the retina. The proper blood supply prevents the damaged blood vessels from being replaced with new ones since the retina is incapable of creating new blood vessels.

e. Non-Proliferative DR (very severe):

The advanced form of DR is called proliferative retinopathy. The newly developed blood arteries here will be weak and erratic. Consequently, bleeding occurs, leading to impaired vision and eventually total blindness. There are two types of diabetic retinopathy: proliferative DR (PDR) is brought on by the growth of new blood vessels in the retina, and non-proliferative DR (NPDR) is brought on by the damage to existing blood vessels brought on by diabetes. [32].

A sample of DR stages images is provided in Figure 2.5.

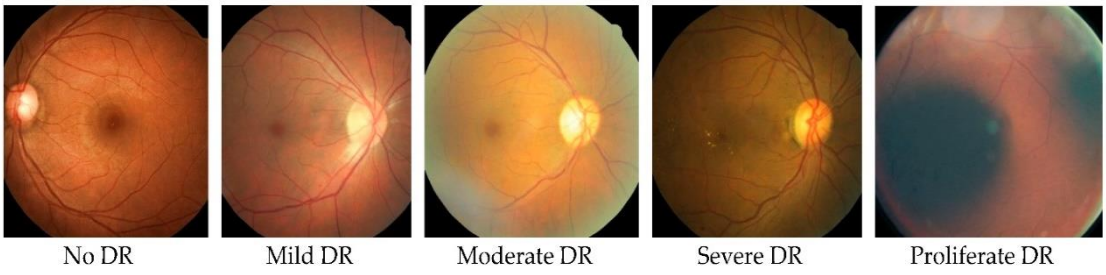


**Figure 2.5:** diabetic retinopathy stages [32].

## 2.5 ARTIFICIAL INTELLEGNECE

Artificial intelligence (AI) methods are commonly used in broadband oscillation research. Machine learning, which imparts intelligence onto computers, deep learning, which mimics the profound thinking of the human brain, and intelligent optimization algorithms, which are based on the principles and structures found in nature and biology, are all examples of such techniques. The foundation of artificial intelligence is machine learning, which enables computers to mimic the way people acquire skills and improve their performance via trial and error [34]. As standard machine learning's shallow structure can't handle the generalization required to tackle complicated problems in the real world, deep learning with its many hidden layers has become a hot topic in the academic community. When it comes to dealing with challenging nonlinear situations, deep learning thrives because of its ability to automatically execute feature extraction via the use of unsupervised learning. Typical applications of deep learning techniques include convolutional neural networks (CNNs) and deep belief networks (DBNs). Algorithms for deep reinforcement learning and deep transfer

learning have emerged as a new branch of artificial intelligence research thanks to the convergence of deep learning, reinforcement learning, and transfer learning. [35]

## 2.6 ARTIFICIAL INTELLENGENCE FOR IMAGE PROCESSING

Image and video data may provide special challenges for analysis. Experts in the medical sector need years of training to be able to spot medical occurrences. In addition, when new information on artificial intelligence's growing role in the medical field becomes available, they will need to actively learn it. When discussing how we classify photos, we may choose to zero down on certain parts of the image and compare those parts to typical parts of images from a given class. This kind of reasoning is routinely used by professionals when faced with difficult identification tasks, such as when radiologists detect cancer by comparing potential tumours on X-rays with prototype tumour pictures [36]. Since it is estimated that high-definition video can store 25 times as much information as high-resolution diagnostic photos like CT, it has the potential to provide a greater data value in the long run. Clinical video analysis has great promise, but is still in its infancy. For instance, a recent study of a laparoscopic operation showed that real-time video analysis could accurately identify each stage of the process (with a 92.8% success rate) and detect any unexpected or unexpected developments. [37] Computers are unable to tell the difference between different sets of pictures since they only know two types: raster and vector. Raster pictures, a kind of bitmap, have each pixel of an image laid out in a grid rather than being randomly distributed. Conversely, vector pictures are made up of polygons that have been assigned colour descriptors. Classifying each picture and specifying its physical properties is essential for data management. Creating picture recognition algorithms needs extreme care since even a small deviation from the norm might make the whole model unusable. The image recognition algorithms then utilize the deep learning datasets to look for such patterns in the images. These data sets include thousands upon thousands of photographs with labels. The program learns what a typical picture of a given item should include by analysing these samples.

## 2.7 NEURAL NETWORK

Artificial Neural Networks (ANN), A convolutional network that may be used for classification is an artificial neural network (ANN). In order to learn, it stores information over time. This quality makes them useful for categorization purposes. For the categorization of SL, read Rahul D Raj et al. [38]'s proposal of ANN. In addition to a parametric vector, the ANN provides a functional one. The data-driven parametric vector is generated by maximum likelihood estimation. The resulting functional shape will be semi-parametric. To fine-tune the model's output, ANN classification takes use of a nonlinear decision boundary. Because of this, the accuracy of the categorization is enhanced in a live environment. Over-fitting is a possible issue with ANN. Artificial Neural Networks (ANNs) are among the simplest types of neural networks, often consisting of only three layers of neurons (input, hidden, and output). If a neural network has just one hidden layer, it is considered shallow (feed-forward). In contrast, the number of hidden layers in a Deep (Feed-Forward) Neural Network (DNN) is more than two. As can be seen in Figure 2.6, all of the artificial neurons that make up the input, hidden, and output layers are connected to one another through connection connections [39]

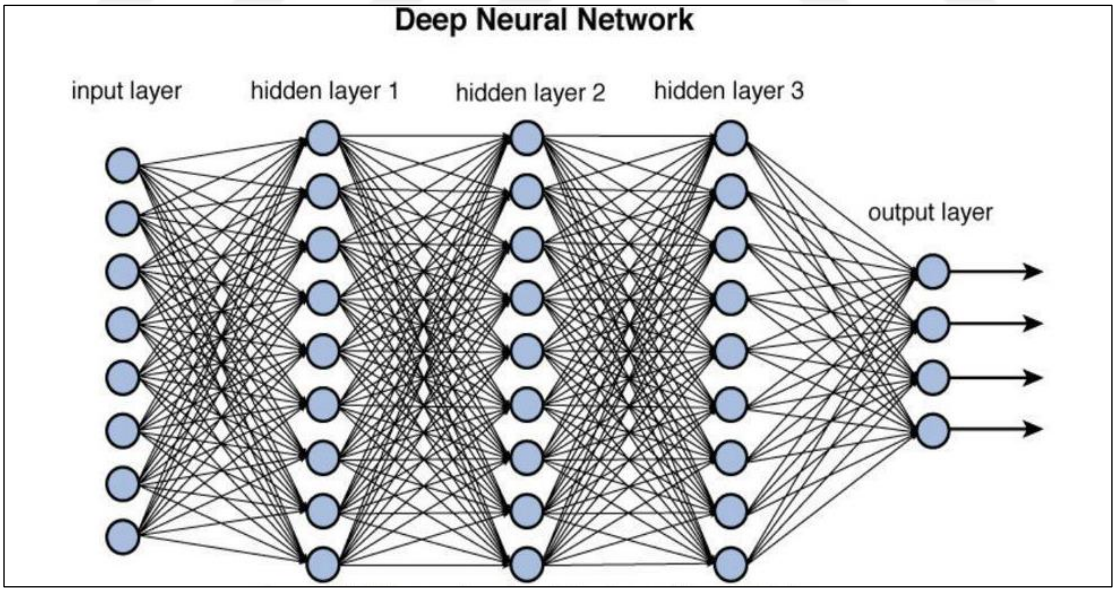


**Figure 2.6:** Deep neural network [39].

## 2.8 NEURAL NETWORK IN HEALTH CARE APPLICATION

Big data and machine learning are changing almost every element of modern life, from the arts and commerce to medicine and even the military. has the capacity to foresee developments in healthcare. The healthcare business stands to benefit greatly from the use of AI technology, which has the ability to enhance every step of the process, from diagnosis to treatment. AI algorithms are performing at or above human levels in several fields, including the interpretation of medical pictures and the linking of symptoms and biomarkers from electronic medical records (EMRs) with the diagnosis and prediction of disease [40].

There is a continuous need for medical treatment, yet many countries lack sufficient medical personnel, especially physicians, to meet that demand. As with other industries, healthcare providers are finding it difficult to keep up with rapid changes in technology and the rising bar set by their patients for both service and outcomes. [41] Artificial intelligence (AI) driven innovations in reducing medical technology are starting to get attention from the medical environment. Experts believe that AI can improve healthcare's administration and distribution operations. It is expected that this would reduce the need for medical care overall. Artificial intelligence (AI)-based technology will play a pivotal role in supporting individuals in preserving their health via constant monitoring, therefore facilitating earlier diagnosis, individualized therapies, and more successful follow-ups. Artificial intelligence in healthcare is expected to see rapid development and reach 6.6 billion by 2021, a CAGR of 40%. [42] Medical personnel may benefit from the use of artificial intelligence in a number of different areas, including general office work, patient contact, and paperwork, as well as in more specialized areas like image analysis, device automation, and monitoring. The best ways to put AI to use in healthcare are still up for discussion. Forbes predicted that in 2018, the most pressing concerns will be on office processes, imaging analysis, robotic surgery, telehealth, and clinical decision support. [43]

## 2.9 NEURAL NETWORK FOR RETINOPATHY DIABETIC DISEASE CLASIFICATION

Researchers have always placed a high value on accurately identifying and diagnosing retinal illnesses at their earliest stages. Attempts at retinal image classification using

conventional machine learning methods have met with some success. On the other hand, DL (Deep Learning) methods have been very effective in the treatment of retinal disorders [44]. A DR screening method that is both automated and capable of making a correct diagnosis quickly is urgently needed. Many methods, including a novel unsupervised technique, have been explored in the attempt to create a highly accurate system. To isolate the fovea from the rest of the retina, deep learning-based techniques are utilized to detect exudates at the pixel level. The first application of CNNs was for image classification. Subsequently, several approaches are used in order to deal with a number of practical issues involving the eyes [45], one of which is the detection of retinal images. In deep learning, CNNs are a form of neural network with several layers of neurons. Neurons in one layer are connected to those in the next through synaptic connections. CNN has several applications in the field of image classification. A characteristic of diabetes is the abnormal growth of blood vessels in the eyes. To establish a correct diagnosis, ophthalmologists must first identify the retinal vasculature's branching network. A typical classification procedure begins with pre-processing, in which segmentation of eye fundus scans is performed so that the branches may be seen more clearly. As such, fundus imaging is often used to diagnose DR. [46]

Image classification may be impaired by problems with lighting and contrast brought on by different approaches of pre-processing images. Categorize the collection of retinal images to detect retinopathy in its earliest stages. In order to enhance the contrast of the pictures, adaptive histogram equalization might be used as a pre-processing step. [47]

# 3. SIMILAR WORK

## 3.1 INTRODUCTION

In this chapter, similar applications will be introduced and discussed. Designed techniques for the methods employed to accomplish the objective and its results.

## 3.2 RANDOM FOREST AND FRACTAL ANALYSIS FOR GRADING DIABETIC RETINOPATHY

Farrikh Alzami [48] reported a study using fractal dimension to differentiate between healthy volunteers and patients with diabetic retinopathy, and between patients with varying degrees of diabetic retinopathy. He used the MESSIDOR dataset with a Random Forest classifier to find that fractal dimensions can distinguish between healthy people and those with diabetic retinopathy

### 3.2.1 Methodology

Due to its ability to offer consistent contrast between structures in fundus images, the green channel is isolated from RGB images during pre-processing. After that, pixel-level characteristics are calculated. After processing, we discard all but the largest 100-pixel-or-larger binary connections. A morphological closing using a disk-shaped structuring element with a radius of 2 pixels is applied to close off any openings in the main arteries caused by the central reflex and reconnect the separated components with the vascular system. Pathological regions are preserved by keeping all connected components with a size greater than 200 pixels. The similarities between fractal objects are measured by what are known as "fractal dimensions," which can be viewed as:

$$D = -\lim_{r \to 0} \frac{\log N(r)}{\log r} \tag{3.1}$$

As an example of an equation for the box-fractal dimension:

$$D_{inf} = -\lim_{r \to 0} \frac{\log Sh(r)}{\log\left(\frac{1}{r}\right)} \tag{3.2}$$

information-fractal dimension can be seen as:

$$D_{inf} = -\lim_{r \to 0} \frac{\log Sh(r)}{\log\left(\frac{1}{r}\right)} \tag{3.3}$$

$$Sh(r) = -\sum_{i-1}^{n_r} p_i(r) \log p_i(r) \tag{3.4}$$

$$p_i(r) = \frac{q_i(r)}{M} \tag{3.5}$$

When everything has been done, correlation dimension can be understood as:

$$D_{cor} = -\lim_{r \to 0} \frac{\log Corr(r)}{\log\left(\frac{1}{r}\right)} \tag{3.6}$$

$$Corr(r) = \frac{i}{{n_r}^2} \sum_{i=1}^{n_r} \sum_{i \neq i} \theta(r - \|p_i - p_j\|) \approx \sum_{i=1}^{n_r} p_i^2(r) \tag{3.7}$$

### 3.2.2 Results

Results for determining how severe a case of diabetic retinopathy was were not sufficient (grade level). Thus, univariate, multivariate, and other statistical aspects are future directions that need to be explored. As a means of learning more about the severity of diabetic retinopathy, it must also focus on the detection of red lesions.

## 3.3 CNN AND SVM FOR IMAGE CLASSIFICATION OF DIABETIC RETINOPATHY AND NORMAL RETINA

Using deep learning and the support vector machine, Dinial Utami [49] suggested a method for extracting and classifying features. High-level characteristics extracted from a CNN's last fully-connected layer are used as inputs to a support vector machine for classification.

### 3.3.1 Methodology

When combined with transfer learning and fine-tuning parameters, CNN has quickly become the gold standard for visual feature extraction. The deep learning transfer learning

frameworks VggNet, Alexnet, InceptionNet, GoogleNet, DenseNet, and Resnet are employed in this research. When it comes to diabetic retinopathy classification, The feature vector for SVM is obtained by transfer learning, and we compare the obtained results to decide whether transfer learning approach is superior. The classification layer is removed and replaced with a fully-connected output layer to get features for the support vector machine classification procedure (SVM). The usual components of a convolution neural network (CNN) architecture are the convolution layer, the pooling layer (also known as a subsampling layer), the fully connected layer, and the classification layer. Example 3.1.

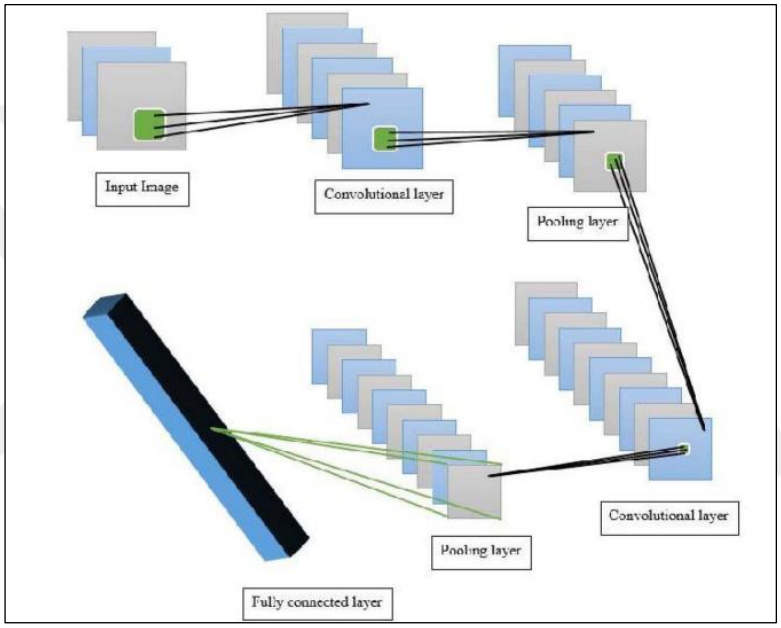


**Figure 3.1:** Architecture of CNN [49].

### 3.3.2 Results

The approach uses CNN with fine-tuning to speed up the classification process and decrease the amount of time needed for the calculation. Seventy-seven base-12 and base-13 retinal pictures from the Messidor database are used to evaluate the suggested approach. The greatest levels of accuracy obtained in the study were 95.83 percent for base 12 and 95.2 percent for base 13, respectively.

## 3.4 RECOGNIZING DIABETIC RETINOPATHY BY COUNTING MICROANEURYSMS IN A COLOR FUNDUS PICTURE

Shailesh Kumar [50] Numerous strategies have been presented for finding and diagnosing DR. Both the total number of MA and their total surface area are included in this research. At first, he employed pre-processing methods such as green channel extraction, histogram equalization, and morphological procedure. The averaging filter, morphological process, principal component analysis, and contrast limiting adaptive histogram equalization have all been used to detect microaneurysms.

### 3.4.1 Methodology

As shown in figure 3.2 The first step in any diabetic retinopathy detection system is pre-processing the fundus image in order to improve contrast. The green channel is widely used in pre-processing because it displays the best vessels/background contrast and the greatest contrast between the optic disc and retinal tissue. The red channel is rather bright, allowing us to see out the choroid's vascular framework. Vascular networks in the retina are also discernible, but with lower intensity than in the green channel. When trying to remove the noise in the blue channel, a mathematical morphological procedure is used. As a part of the microaneurysm identification method, a closed-loop enhancement (ADHE) is applied to a pre-processed green channel picture to eliminate noise from the object region. Following this step, blood vessel extraction is performed.

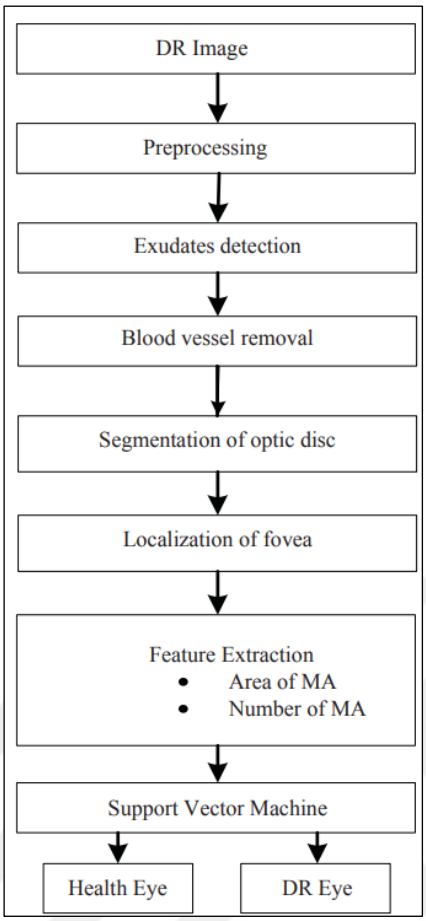


**Figure 3.2:** Detection Process of DR [50].

For feature extraction Microaneurysms have two distinguishing features: the size of the lesion and the presence of a thrombotic process. Fundus pictures have been analysed for microaneurysms and the total number of MAs present. Microaneurysm area is determined by counting the amount of white pixels in the extracted picture, as seen in Figure 3.3. A microaneurysm is counted as the number of sudden transitions from white to black pixels.

**Figure 3.3:** Microaneurysm Extracted From Fundus Photo [51].

The SVM classifier has been used to diagnose DR. SVM split the picture in half, say, between DR eyes and healthy ones. eye. The SVM classifier's parameters have been determined using signs and symptoms of a microaneurysm. minimally dimensional). The area of MAs and the total number of MAs were used to fine-tune the SVM's input features throughout the training process. The parameters of a Support Vector Machine (SVM) have been trained using a linear kernel with fivefold validation, and the average number and area of microaneurysms are employed as the classification threshold. The SVM classifier is improved by providing it with additional testing data after it has been trained.

### 3.4.2 Results

A linear Support vector machine classification method has been used to DR (SVM). It has been shown that the DR detection method has a sensitivity of 96% and a specificity of 92%. As may be seen in figure 3.4 a DR diagnostic yielded the expected outcome. 10. The DIABETDB1 picture database has been culled for 110 photos. Fifty-eight of the photos are utilized for the training sample with five-fold validation, and fifty-two are used for the testing sample. It is clear from figure 3.4 that the linear SVM classifier can reliably categorize six testing samples. MATLAB R2015a was used for the simulations. The effectiveness of the suggested method for DR detection is measured in terms of its sensitivity and specificity.

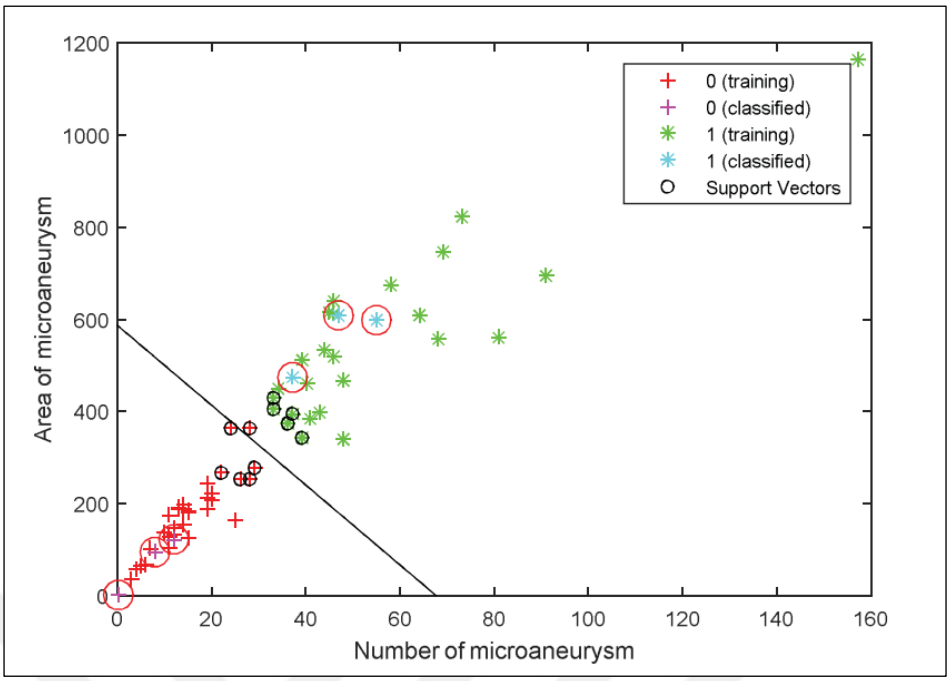


**Figure 3.4:** Testing and Training Image Results [51].

## 3.5 COMPARISION

In this section, a comparison of similar applications will be shown in detail including the author, methodology, dataset and its results:

**Table 1.1:** Analysis of the Similar Studies [51].

| **Application name and Author** | **Dataset used** | **Methodology** | **Usability and Result** |
|---|---|---|---|
| Kumar, S., & Kumar, B. (2018). Diabetic Retinopathy Detection by Extracting Area and Number of Microaneurysm from Colour Fundus Image | One hundred ten images (normal images and abnormal images) have been taken from DIABETDB1 database. | Linear use of SVM | suggested a method for better non-invasive diabetic retinopathy (NPDR) detection by calculating the area and number of microaneurysms in DIARETDB1 color fundus images. Preprocessing of Fundus Images |
| Alzami, F., Abdussalam, Megantara, R. A., Fanani, A. Z., & Purwanto. (2019). Diabetic Retinopathy Grade Classification based on Fractal Analysis and Random Forest | MESSIDOR dataset for fractal analysis | MESSIDOR dataset and Random Forest as Classifier and fractal analysis | Simple to use for identifying normal eyes and those with diseases |
| Qomariah, D. U. N., Tjandrasa, H., & Fatichah, C. (2019). Classification of Diabetic Retinopathy and Normal Retinal Images using CNN and SVM | Messidor database has 77 photos of the retina from base 12 and 70 images from base 13 | SVM and ANN | With base 12, inception v3, and VGG Nettype 19, they reported an accuracy of 95.83%.gave the accuracy of 95.24% for base 13 |

# 4. METHODOLOGY AND RESULTS

## 4.1 CONVOLUTIONAL NEURAL NETWORK TECHNOLOGY

It is one of the most significant neural networks that was developed utilizing the technique of deep learning [51], and its purpose is to recognize and monitor biological activities. It does this by simulating the processes that take place in the many levels of a human brain while genuine cognition is taking place.

Deep Neural Networks (DNNs) are taught differently from Convolutional Neural Networks (CNNs) in terms of what they learn, how they evolve, and how they are constructed. It is possible that it might be considered a kind of network data due to the fact that it manages information such as picture data. The data that is processed by the network can have either a two- or a three-dimensional structure, and it will thus contain pixels.

CNN is able to classify and recognize items depending on their orientation and the direction in which they are being viewed since it is based on computer programs and functions within those programs. CNN may analyse the data and the images to identify what they are using certain features. The modelling capabilities of CNN techniques are far greater than those of other approaches, which allows these methods to derive more value from the data than other methods. CNN is able to recognize disease and classify it into a variety of phases and degrees by conducting an analysis of the properties of medical photographs [52 , 53].

The process that is referred to as convolution is part of what is known as a convolutional neural network (CNN), which is a type of neural system that comprises hidden layers that are capable of extracting a variety of attributes from images and also includes a layer for the output.

CNN views a picture as a three-dimensional matrix that is composed of colour pixels (width, height, and depth) that each have a value that ranges from 0 to 1. (0 - 255) If the user uploads a photo that contains colours, the colours will be distributed evenly over the width and length of the image. On the other hand, there is just one-color channel in a grayscale image.

The amazing architecture of CNN, which consists of a number of different layers, is the source of the network's powerful capacity to recognize successfully. It is made up of one

pooling layer, one convolution layer, and one fully connected layer—all of which are hidden layers—with the final product being referred to as either an activation or a feature map, depending on whether or not it is being utilized as an input to another layer [54]. The first layer also contains a variety of filters that may be used to apply to images in order to extract high or low qualities, such as the presence of blood vessels or the lack of particular edges and curves. These filters can be applied to photos in order to extract high or low qualities. As a consequence of this, CNN is in a position to detect certain patterns and edges that a human brain would ordinarily be unable to do so due to the advanced algorithms that it employs.

So, the operational notion behind these layers may be investigated in greater depth, initially on their own and then together. The convolutional neural network (CNN internal)'s hidden layers are in charge of a range of important functions that take place within the network's neural architecture. Use of this network contributes to overall cost savings, which benefits all activities. When all of the neurons of the CNN have been completely active, the hidden layers of the neural network will start to perform their functions. A convolutional neural network, often known as a CNN, has minuscule units within each neuron that are solely devoted to doing mathematical calculations and putting those calculations into action. Communication with other neurons is the fundamental purpose of this neuron [55]. The following figure 4.1 presents a representation of the concealed layers.

A convolutional neural network (CNN) that is arranged in three dimensions (length, width, and depth) and in which each layer starts with input processes before moving on to other layers to prepare for output processes where the neurons begin activating and converting the 3D input to the 3D output of neurons [56]. The length, width, and depth of the CNN are measured in units of length, width, and depth, respectively. Hence, this process is illustrated in Figure 4.2.

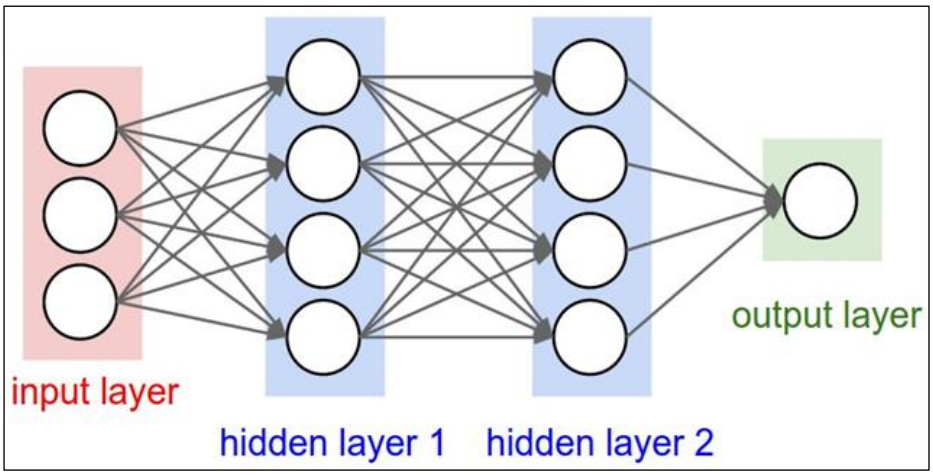


**Figure 4.1:** CNN and Its Hidden l.

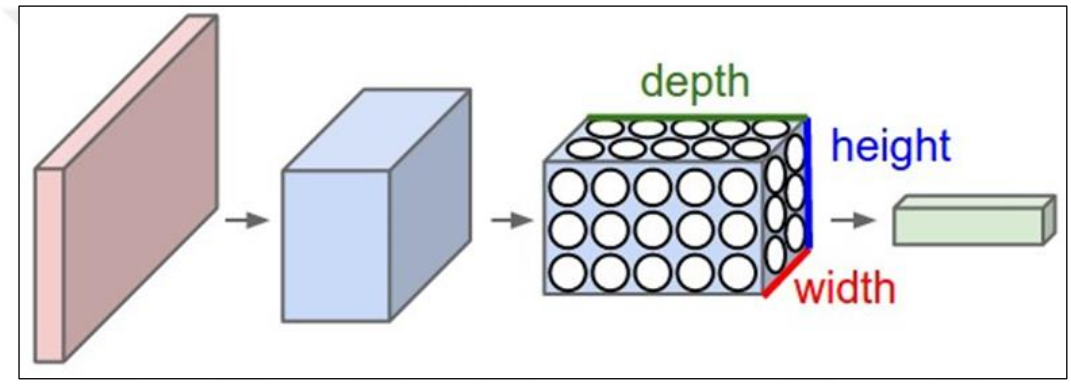


**Figure 4.2:** Illustrate a 3D CNN.

### 4.1.1 CONVOLUTIONAL LAYER

There is a great deal of consensus among experts that the convolutional layer is the most important component of a CNN [56]. It does this by stacking layers on top of each other and using the findings from these stacked layers as the basis for its hypothesis in order to extract more specific traits. The full correlation layer may be able to conduct a two-way conversation with the pixel in the receiving field, but the convolutional layer is unable to do so since it is not connected in the input picture. This layer is responsible for the beginning of the feature processing and mostly provides assistance with calculating and locating features. The CNN's sliding window convolutional feature is able to successfully eliminate features from the input image. This is made possible by first optimizing the picture.

CNN gives more priority to the low-level characteristics in the first hidden layer before integrating them into higher-level features in the second hidden layer and so on [56]. This is

due to the fact that the neurons in the second convolutional layer are linked to the neurons in the first. One of the most important advantages of the convolution layer is that it may go exceptionally deep into the volume input layer because to the many filters known as kernels that it contains.

This is due to the fact that, in the same way as the other hidden neurons, these filters also have weights. At each iteration of the training process known as "squeezing," the filters start the process of looking for new characteristics in the input picture that they have been given (epochs). Implementing the convolution filter via the input, where the matrix is multiplied at each point, and the result is recovered and gathered on the feature map [56] is required in order to build the feature map after the filter or kernel has convolutionally processed the input data. The op convolution technique is depicted in Figure 4.3. The green filter (squares) are slid over the blue input (squares), and the result is summed and added to the feature map in the small square on the right.

If the size of a filter is kept constant at 1, then every pixel-by-pixel movement that occurs during the STRID process may be completed with a single pass [56]. If the filter sliding step is more than a single pixel on the input, then the stride will become more significant [56]. When the size of the input is greater than the size of the feature map, the feature map needs to be shrunk; however, there is a way to prevent this by using padding; in this case, a layer containing zero values will be added so that the input layer is surrounded by this new layer of zeros; this prevents the feature map from shrinking and also preserves the spatial size when performing the convolution operation and improves performance. Padding can be used to prevent the feature map from shrinking when the size.

The feature map is generated as soon as the convolutional layer completes its analysis of the available data. CNN uses the activation function to make the output non-linear after the convolution, and the activation function that is used is ReLU to transfer the weighted results and outputs from the convolution [56]. The following is an illustration of a ReLU function example: (Equation 4.1 and Figure 4.4).

$$F(z) = \max(0, z) \tag{4.1}$$

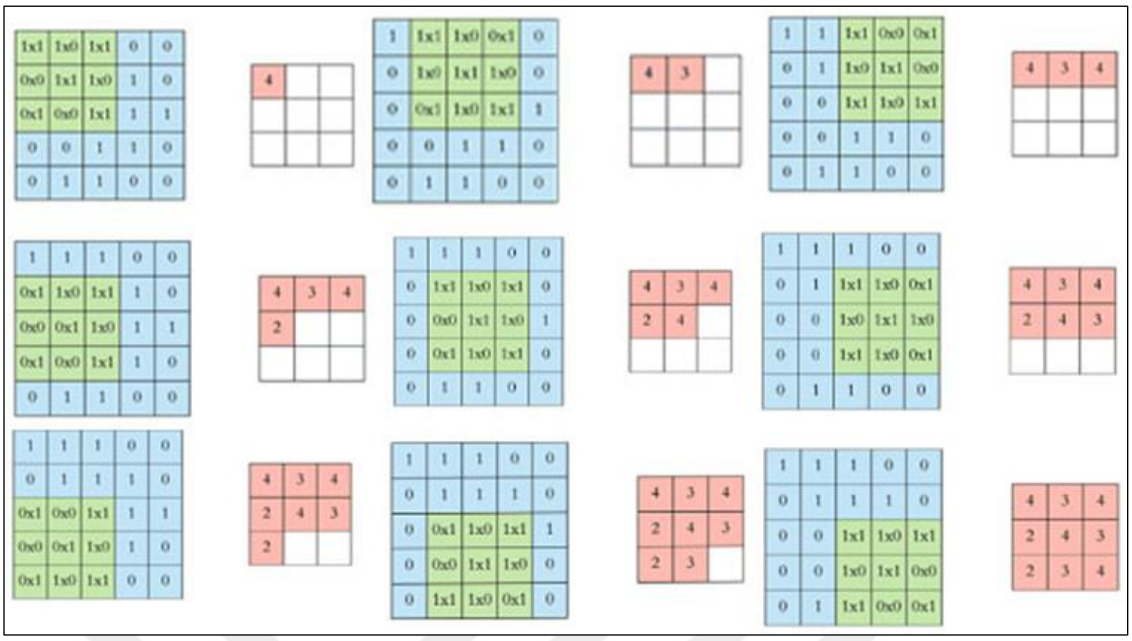

**Figure 4.3:** Illustrate Sliding the Filter.

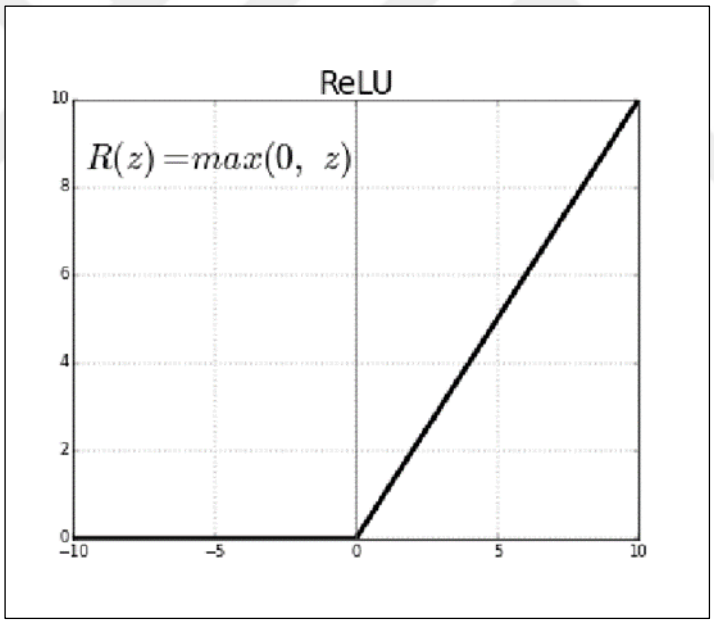


**Figure 4.4:** RELU Function.

The original approach works in a three-dimensional matrix that includes width, height, and depth; however, for the sake of clarity, the description will focus on the two-dimensional version of the method. When a visible feature, edge, speck, or colour spot is identified, the filters in the CNN are engaged, and it begins learning that particular feature. After that, each filter generates a distinct two-dimensional output feature map, and this process continues

until a sufficient number of these feature maps have been aggregated and integrated so that a single output volume may be generated. A graphical illustration of this procedure may be seen in Figure 4.5, which is presented here.

CNN's filters commonly apply 2D convolutions to both the data and the images they process. As can be seen in the following graphic, the filter will continue to move in both the X and Y directions until the image's dimensions have been calculated (Figure 4.6).

The following equation may be created by using variables such as D, which stands for the number of output layers, W, which stands for the real number, P, which stands for the total volume of the warp pad, K, which stands for the size of the kernel, and S, which stands for the stride size [57].

$$D = \frac{[W-2P-K]}{S} + 1 \tag{4.2}$$

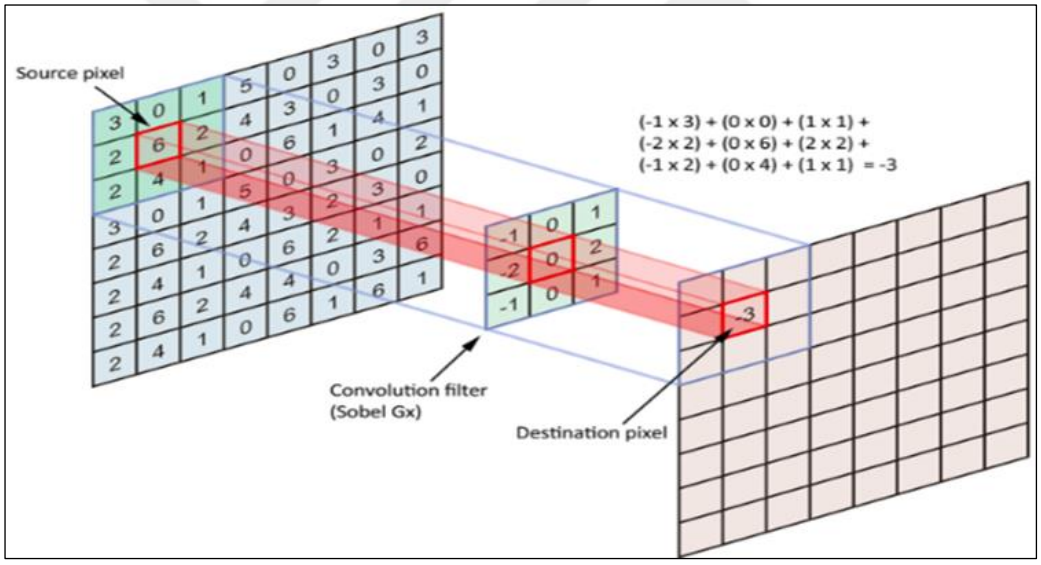


**Figure 4.5:** Operation on the Input to be Output to a New Layer.

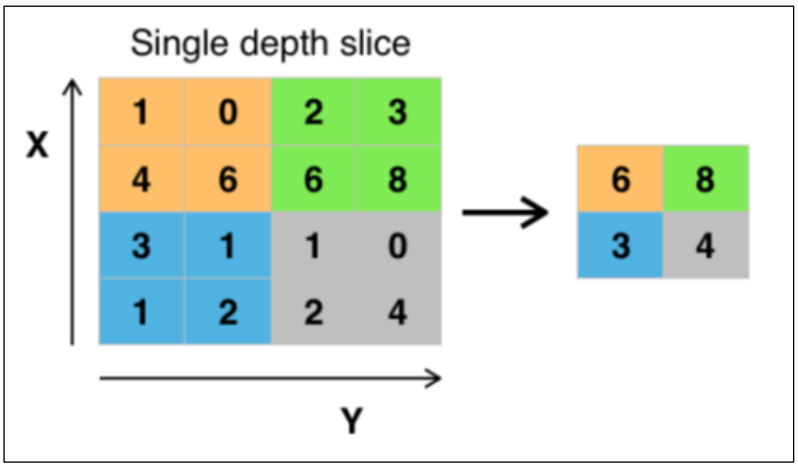


**Figure 4.6:** 2D Convolution (X, Y) Without Depth.

### 4.1.2 POOLING LAYER

A further component of CNN concepts is the pooling layer, which is a non-linear model of its own kind. The maximum pooling layer is by far the most popular and widely utilized of the various helpful non-linear pooling layers that are available. The pooling layer begins its work by taking samples from the feature map in order to provide the highest possible output. To do this, it first divides the picture into a number of rectangles. Each neuron in this layer is only able to communicate with a small subset of neurons in the layer that lies below it (pooling layer). In addition to this, there is no requirement for the use of weights because it may accomplish its own function. The pooling layer is the one that takes the inputs from the layer below it and begins to minimize the calculations that are taking place within the network [56]. This is done for the reasons that have been mentioned above, as well as to reduce the locative volume of the input pictures, overfitting, and memory use. Both MaxPooling and AvgPooling are functions of aggregating neurons, and they are shown in Figure 4.7 below to illustrate how the pooling layer technique works.

Even when employing 2 * 2 kernels and 2 stride, the output will be squared in both directions when more than half of the inputs are projected via the pooling layer. This is due to the fact that the pooling layer is a high reduction layer. There will be no alteration to either the width or the height of the inputs. The depth channels of the network are reduced by this layer, which makes it possible for the majority of neurons to be grouped along the width and height

axes instead. The mathematical formula for both MaxPooling and AveragePooling may be found in this equation (4.3).

$$D = \frac{[W+P]}{S} + 1 \tag{4.3}$$

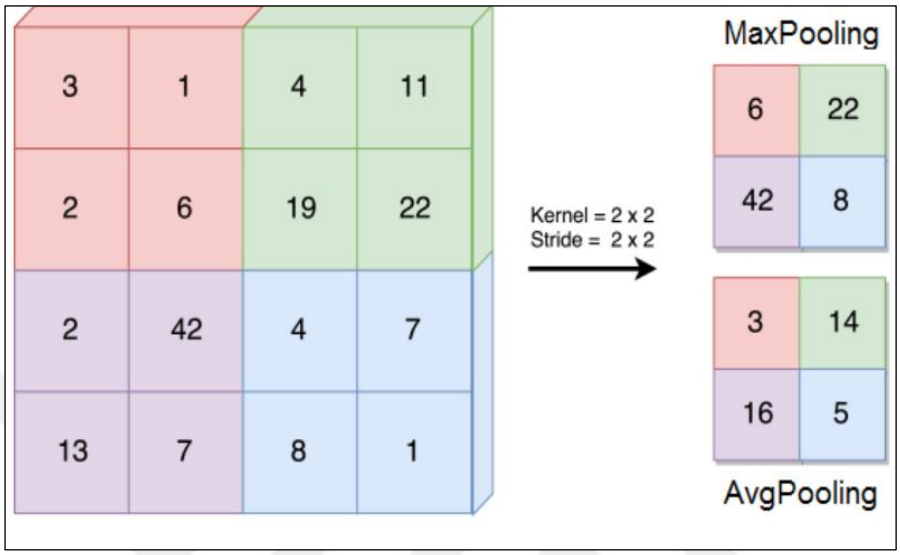


**Figure 4.7:** MaxPooling Layer, AvgPooling 2*2 no Padding.

### 4.1.3 FOLLY CONNECTED LAYER (FC)

The CNN architecture utilizes a final layer called the fully connected layer [58], which has the function of smoothing down the output of the preceding layers and turning it into a 1D array. This layer is there despite the fact that the Convolutional and Pooling layers are rather deep. The last layer of a CNN contains the classifier for the network. This layer is made up of neurons that are connected to cells in the layer above it. The final output will be the CNN's final output once this layer is finished being processed. The levels that come before the fully linked layer in the network provide the input for this layer, which is also referred to as a feature map. As visuals from lower layers are brought up, the neurons in this layer utilize their sense of touch to draw judgments about what is going on in the settings that are being shown to them. Figure 4.8 can help you better comprehend what a layer is.

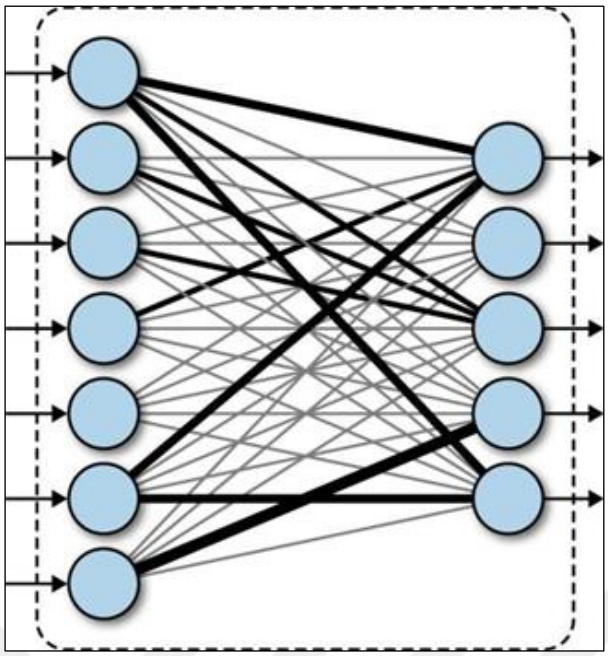

**Figure 4.8:** The Folly Connected Layer.

### 4.1.4 CONVOLUTIONAL NEURAL NETWORK ARCHITECTURE

For instance, the first layer initiates the process of inserting an image into it by extracting its properties, the second layer initiates the process of assembling (pooling), and the final layer (classifier) initiates the process of shrinking the outputs, all while remaining connected to one another. The construction of a convolutional neural network (CNN) looks like this. A CNN performs analysis on the input picture by utilizing a number of layers, each of which has a distinct quality in terms of the operations that are performed on it. Figure 4.9 illustrates a convolutional neural network's fundamental building blocks in terms of its architecture.

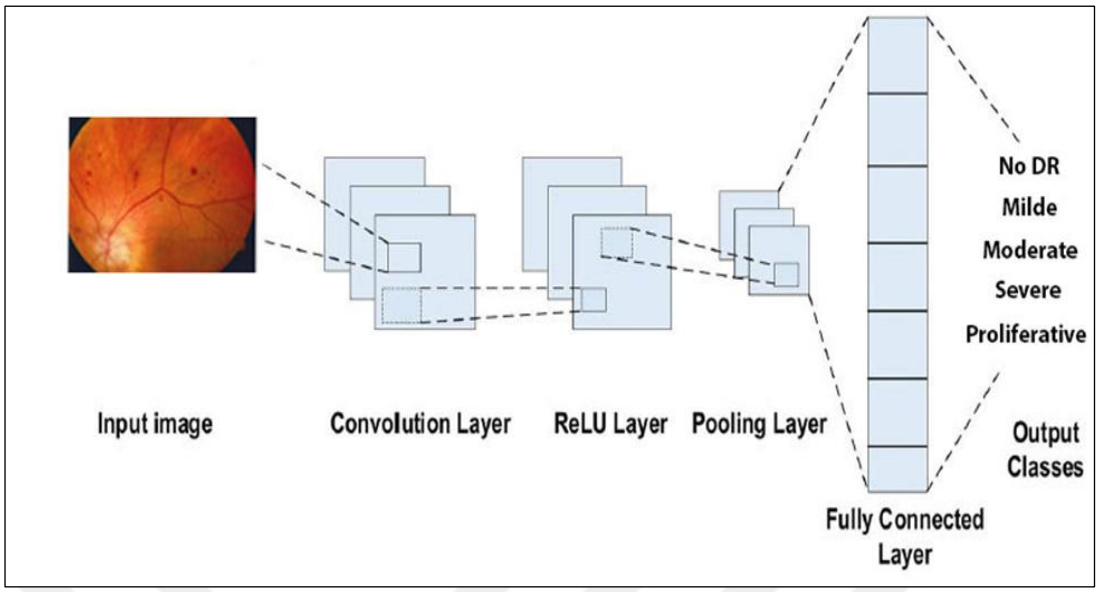


**Figure 4.9:** CNN Architecture.

## 4.2 IMPROVEMENT ALGORITHMS FOR TRINING NEURAL NETWORKS

In this part, we will discuss some of the most important optimization algorithms, such as stochastic gradient descent, Adam, and Rmsprop. These algorithms are all used in the process of teaching neural networks how to learn new information, thus it is important that we understand them. In this particular scenario, we make use of dropout in conjunction with batch normalization [59-61]. Improve the model's accuracy while at the same time reducing the loss function it produces. When optimizing over several data instances, the metric that you should be aiming for is the average loss.

### 4.2.1 Stochastic Gradient Descent (SGD)

SGD is used to maximize gain while minimizing loss in order to bring CNN weights up to date for more accurate picture categorization. In order to do this, it makes use of a linear combination of the past weights updates Vt as well as the present negative gradient L(W) and takes into consideration both of these factors. The weight W an is proportionate to the total amount that was learned and is determined by applying the minus-L gradient to the calculation (W). displays the rate of change during the period of time that has passed since the previous Vt update. SGD is used to derive the updated value, which represents Vt+1 and the updated weights Vt+1 at repetition T+1, by applying the current weight Wt and the prior

update of the weight Vt, as shown below. This allows for the generation of the updated value, which represents Vt+1 and the updated weights Vt+1 at repetition T+1.

$$V_{t_{+1}} = \mu V_t - a\nabla\mathcal{L}(W_t) \tag{4.4}$$

And

$$V_{t_{+1}} = W_t + V_{t_{+1}} \tag{4.5}$$

### 4.2.2 Root Mean Square Prop(RMSPROP)

The illustrious team of Tieleman and Hinton was responsible for the development of the ADMA optimization method, and they used this variation in their work. The momentum is used to create one-of-a-kind updates, which are then used in the process of rescaling the gradient. The momentum is used to create one-of-a-kind updates, which are then put to use in the process of rescaling the gradient. RMSPROP will choose a new learning rate whenever it is given access to a fresh set of parameters. The tempo of the lesson can be altered in a mechanical way. Due to the fact that there is a unique update for each parameter, the process of updating will now start at this point in accordance with the following equations.

$$(v_t) = p\, v_{t_1} + (1 - p2) * g_t^2 \tag{4.6}$$

$$\Delta\omega_t = -\frac{\eta}{\sqrt{v_t + \epsilon}} \tag{4.7}$$

$$\omega_{t_{+1}} = \omega_t + \Delta\omega_t \tag{4.8}$$

### 4.2.3 Adam

It is a gradient-dependent optimization process that contains an adaptive moment estimation $(m_t, V_t)$. The parameters of the update appear in the following equations:

$$(m_t)_i = \left(m_{t_{-1}}\right)_i + (1 - \beta_1)\ \left(\nabla\mathcal{L}(w_t)\right)_i \tag{4.9}$$

and

$$(v_t)_i = \beta_2\left(v_{t_{-1}}\right)_i + (1 - \beta_2)\left(\nabla\mathcal{L}(w_t)\right)_i^2 \qquad (4.10)$$

Suggest using in[84] $\beta_1 = 0.9,\ \beta_2 = 0.999, and \in = 10^{-8}$ as parameter default values.

## 4.3 PROPOSED METHODOLOGY

Locate all of the spots of the retinal picture that have a high brightness. There is a possibility that the Optic Disk and the Hard exudate patches are located in the bright regions. A technique that is based on active contours was used to analyse the optic disk in digital photographs of the retina. It is an area on the retina that is responsible for the entry and exit of axons from the optic nerve into and out of the eye. Hard exudates can be recognized by their brilliant yellow patches with sharply defined edges and lipid deposits. The fuzzy c-means technique may be used to differentiate between such exudates. The fact that the Optic Disc (OD) is visible in the pictures is one of the most significant issues.

The next step is to locate and isolate the vertical vessels within the picture. If there are vertical vessels in the closest neighbours of the bright patch in a picture, then such patch is identified as the Optic Disk. To put it another way, the candidate that is determined to be the Optic Disk is the one that has the highest total number of vertical vessel pixels that traverse through it. In the photograph of the retina, the bright region that can be seen is the optic disk. It is impossible to see anything through the optic disk since the optic nerve itself is not sensitive to light.

After locating potential possibilities for bright spots in the photos, the Optic Disk is removed from those locations.

The optic disc is the segment of the optic nerve that is located within the eye and may be seen using an ophthalmoscope. The ratio of its cup to its disc, as well as its edges and colour, should be decided. The disc ought to be round or somewhat elliptical, with the long axis generally running vertically, and it ought to have crisp boundaries. In most people, the nasal boundary is very little blurry.

If, following the elimination of the OD in each picture, there are still candidates of bright patches, then those bright patches are recognized as being hard exudates.

With the purpose of identifying the hard exudates, the images are divided into as many as 15 different categories based on the highest value of the color in each image. At a given location, hue (h) is defined as the ratio of the intensities of green (g) and red (r). When an image is provided, the type number will be applied to it.

The suggested process is illustrated in flowchart form in Figure 4.1.

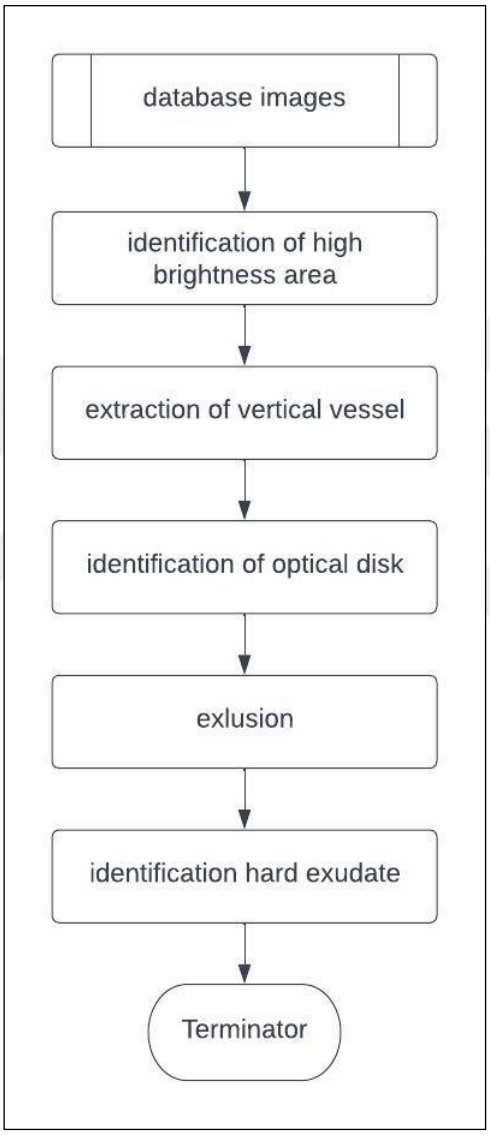


**Figure 4.10:** Proposed Methodology Flowchart.

## 4.4 USED DATABASE

The "INDIAN DIABETIC RETINOPATHY IMAGE DATASET" from Kaggle was used so that the analysis could be carried out. The incidence of diabetic retinopathy is higher than

that of any other kind of blindness or vision loss among the world's population that is of working age. Recent research has increased our knowledge of the essential need in clinical eye care practice for new, cost-effective techniques of detecting, managing, diagnosing, and treating retinal illness. This awareness has improved as a result of the recent studies. Because of the necessity of diabetic retinopathy screening programs and the difficulty of obtaining a dependable early diagnosis of diabetic retinopathy at an affordable price, the development of a computer-aided diagnosis tool is vital. This is because of both of these factors. It is possible that retinal image analysis employing computer-assisted disease diagnosis may make mass screening for persons who have diabetes mellitus easier and will help physicians make more efficient use of their time. Because of recent developments in computing power, communication networks, and methods of machine learning, biomedical engineers and computer scientists now have access to the resources necessary to meet the requirements of clinical practice. For the purposes of development, testing, and assessment, digital screening systems and the automated algorithms that underpin them require huge image sets of the retina that are varied, representative, and of a wide variety of types. The IDRiD dataset, which stands for the Indian Diabetic Retinopathy Image Dataset, is the first database of its sort to be constructed with the intention of being representative of the Indian population. This challenge will use this dataset. In addition, it is the only dataset that labels, at the pixel level, both typical diabetic retinopathy lesions and normal retinal structures. This makes it very useful. Every single picture that is included in this dataset has been determined to have diabetic retinopathy or diabetic macular edema, and the severity of the condition has been rated for every single one of them. Because of this, it is ideally suited for the testing and improvement of image processing algorithms for the screening of diabetic retinopathy.

The training image dataset is comprised of 20,000 32x32 picture patches containing hard exudates at location (17,17), as well as 20,000 similar image patches without hard exudates at position (17,17). (17,17).

Figure 4.2 is an example of the dataset images.

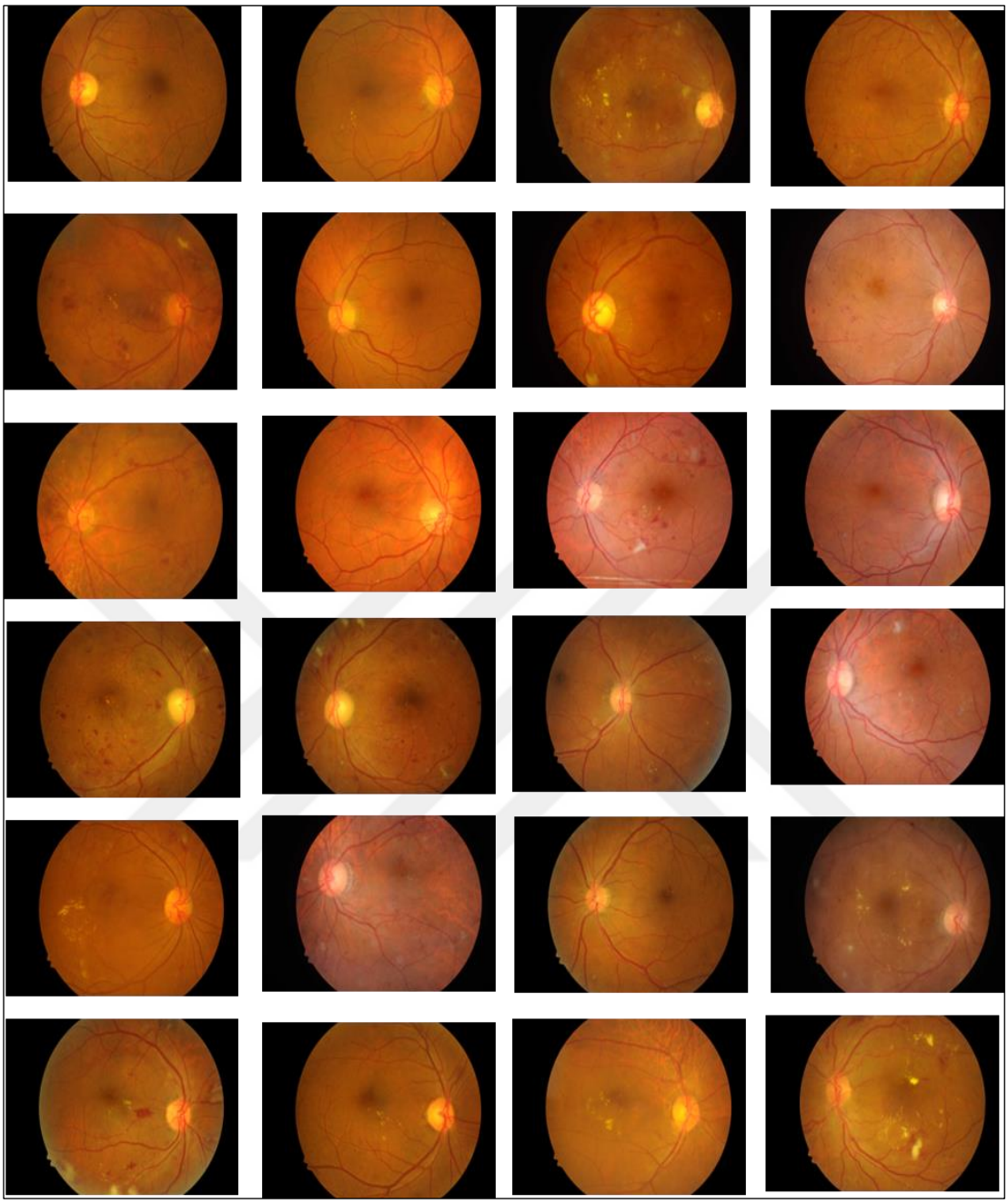

**Figure 4.11:** Dataset Images Example.

## 4.5 ALGORITHM

A system that uses deep learning has discovered that the DR-affected fundus image contains evidence of the existence of hard exudates. It is generally accepted that the intensity of the hard exudates in all retinal fundus photographs is equal to one, whereas the intensity of the backdrop is always thought to be zero.

STEP 1: The first step is to reduce the size of each of the fundus photos to 256 by 256 pixels.

STEP 2: Utilizing the ground truth photographs, locate the pixel of interest at the site, and then cut off a 32x32 patch from those pictures (17, 17). Because the ground truth photographs were not doctored in any way, not every single pixel is being taken into consideration. The resolution of the original photographs is measured on a scale ranging from (16, 16) pixels to (240,240).

STEP 3: In the third step, a convolutional neural network consisting of 8 layers and a 2x2 kernel is employed in order to conduct an analysis of the image patches. The central pixel of an image patch is analyzed by a neural network that has been trained to detect whether or not the patch represents an item or the background.

STEP 4: After every other convolution layer, the Maxpool algorithm is applied to shrink the feature map by a factor of two. This brings us to STEP 4.

STEP 5: When it comes to the speed of training, PHASE 5 comprises the utilization of batch normalization in each and every convolution layer. This is the fifth step.

STEP 6: In order to prevent overfitting, go to step six, which is called "drop out."

STEP 7: In the seventh step of the process, 20,000 photo patches were sorted into 5,000 groups of 40,000 and trained for a total of 500 iterations each. When a network has trained all 40,000 picture patches in a single set for 500 iterations, we say that it has a streak. In the current network, there is already enough data for three complete streaks' worth of training, which adds up to a total of 1500 training epochs.

STEP 8: After the network has been trained on the photographs, the pictures are cut up into 50176 patches, and a guess is made regarding whether or not the central pixel represents a solid item or the backdrop.

STEP 9: The ninth step is to convert these pieces into full-resolution pictures measuring 224 by 224 pixels. This is necessary because padding was not utilized in the creation of these photographs. As a direct consequence of this, photographs of hard exudates are obtained.

## 4.6 RESULTS

After training, the accuracy is equal to 99.74%. Figures below show all the steps. Some comparison with similar work accuracies done in Table 1 show the outperforming of the proposed method among other literature review methods.

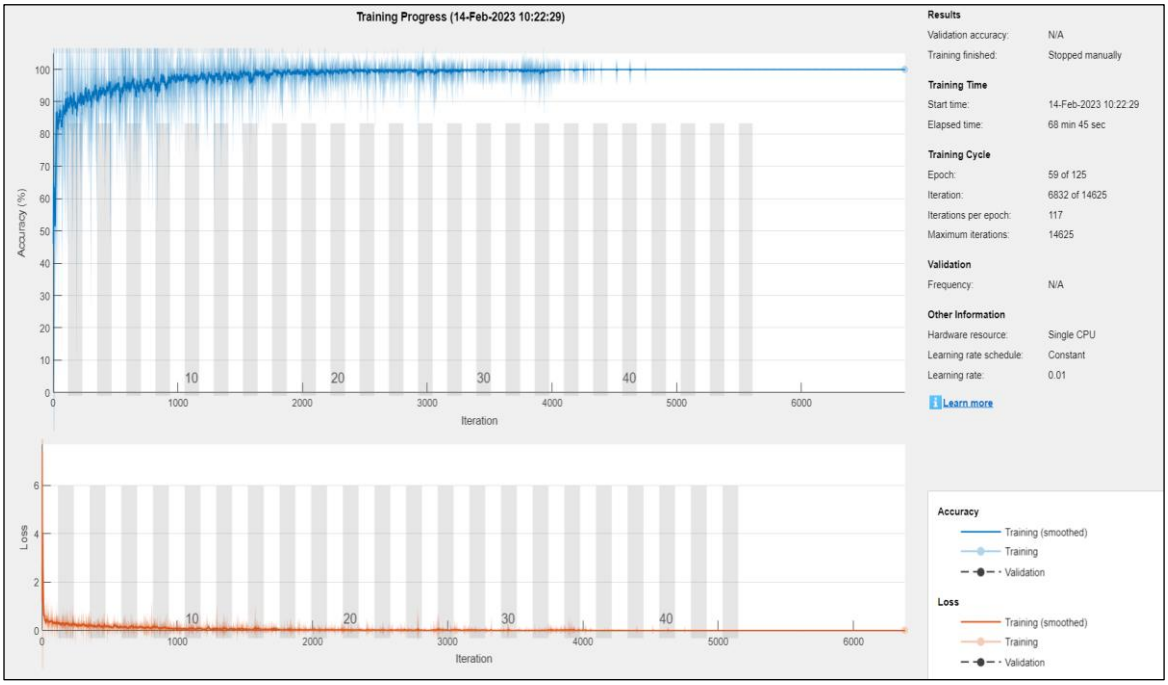


**Figure 4.12:** Training Process.


**Figure 4.13:** Final Iteration of Training.

```
Training on single CPU.
Initializing input data normalization.
|=========================================================================================|
|  Epoch  |  Iteration  |  Time Elapsed  |  Mini-batch  |  Mini-batch  |  Base Learning  |
|         |             |   (hh:mm:ss)   |   Accuracy   |     Loss     |      Rate       |
|=========================================================================================|
|       1 |           1 |       00:00:04 |       49.22% |       1.0670 |          0.0100 |
|       1 |          50 |       00:00:32 |       94.53% |       0.1676 |          0.0100 |
|       1 |         100 |       00:01:01 |       92.19% |       0.1680 |          0.0100 |
|       2 |         150 |       00:01:29 |       98.44% |       0.0416 |          0.0100 |
|       2 |         200 |       00:01:57 |       99.22% |       0.0289 |          0.0100 |
|       3 |         250 |       00:02:30 |       98.44% |       0.0552 |          0.0100 |
|       3 |         300 |       00:03:10 |       98.44% |       0.0652 |          0.0100 |
|       3 |         350 |       00:03:50 |       99.22% |       0.0346 |          0.0100 |
|       4 |         400 |       00:04:30 |       99.22% |       0.0675 |          0.0100 |
|       4 |         450 |       00:05:10 |       99.22% |       0.0089 |          0.0100 |
|       5 |         500 |       00:05:51 |      100.00% |       0.0026 |          0.0100 |
|       5 |         550 |       00:06:33 |       99.22% |       0.0078 |          0.0100 |
|       6 |         600 |       00:07:03 |       98.44% |       0.0250 |          0.0100 |
|       6 |         650 |       00:07:32 |       98.44% |       0.0290 |          0.0100 |
|       6 |         700 |       00:08:01 |       99.22% |       0.0292 |          0.0100 |
|       7 |         750 |       00:08:30 |      100.00% |       0.0049 |          0.0100 |
|       7 |         800 |       00:08:59 |      100.00% |       0.0002 |          0.0100 |
|       8 |         850 |       00:09:27 |       98.44% |       0.1082 |          0.0100 |
|       8 |         900 |       00:09:56 |      100.00% |       0.0013 |          0.0100 |
```

**Figure 4.14:** Steps in MATLAB.

```
accuracy =

    0.9974
```

**Figure 4.15:** Accuracy.

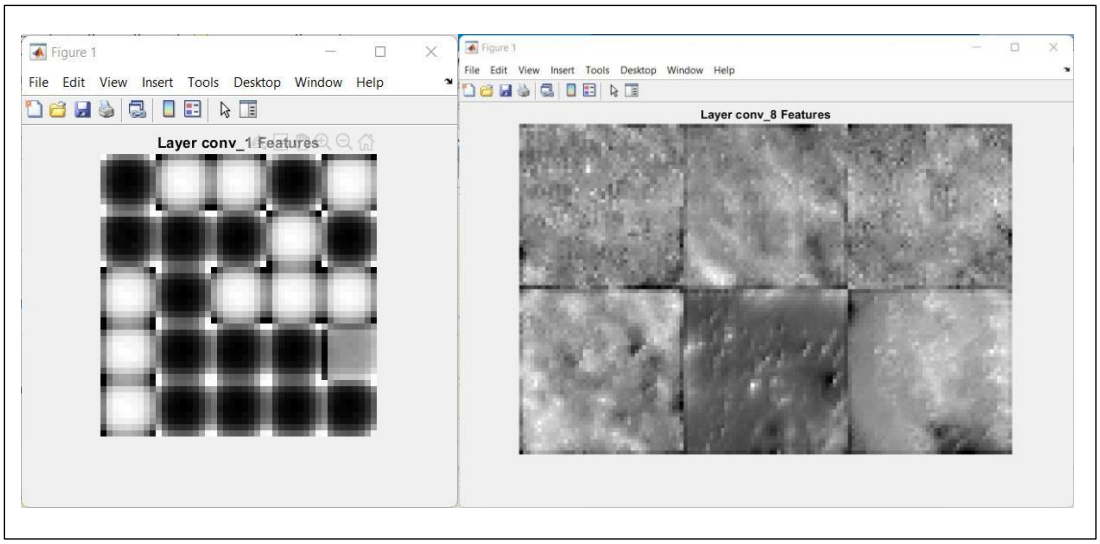


**Figure 4.16:** First and Last CNN Layer.

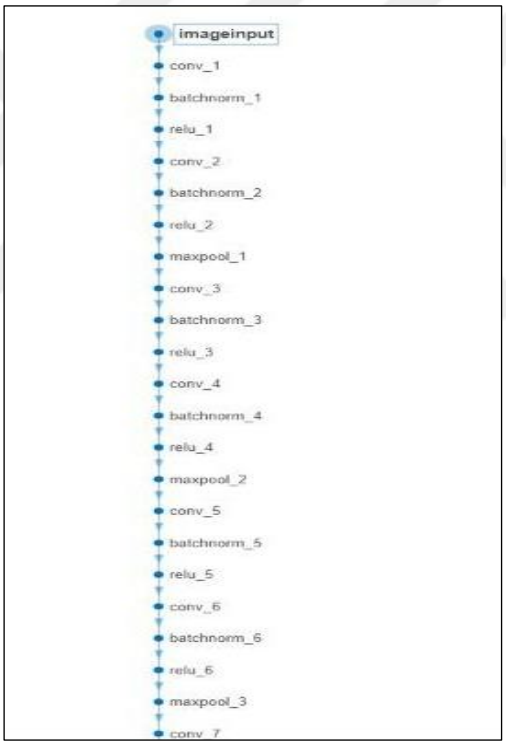


**Figure 4.17:** Proposed Method Architecture.

| | Name | Type | Activations | Learnables |
|---|---|---|---|---|
| 1 | imageinput<br>32×32×1 images with 'zerocenter' normalization | Image Input | 32×32×1 | - |
| 2 | conv_1<br>32 2×2×1 convolutions with stride [1 1] and padding 'same' | Convolution | 32×32×32 | Weights 2×2×1×32<br>Bias 1×1×32 |
| 3 | batchnorm_1<br>Batch normalization with 32 channels | Batch Normalization | 32×32×32 | Offset 1×1×32<br>Scale 1×1×32 |
| 4 | relu_1<br>ReLU | ReLU | 32×32×32 | - |
| 5 | conv_2<br>32 2×2×32 convolutions with stride [1 1] and padding 'same' | Convolution | 32×32×32 | Weights 2×2×32×32<br>Bias 1×1×32 |
| 6 | batchnorm_2<br>Batch normalization with 32 channels | Batch Normalization | 32×32×32 | Offset 1×1×32<br>Scale 1×1×32 |
| 7 | relu_2<br>ReLU | ReLU | 32×32×32 | - |
| 8 | maxpool_1<br>2×2 max pooling with stride [2 2] and padding [0 0 0 0] | Max Pooling | 16×16×32 | - |
| 9 | conv_3<br>64 2×2×32 convolutions with stride [1 1] and padding 'same' | Convolution | 16×16×64 | Weights 2×2×32×64<br>Bias 1×1×64 |
| 10 | batchnorm_3<br>Batch normalization with 64 channels | Batch Normalization | 16×16×64 | Offset 1×1×64<br>Scale 1×1×64 |
| 11 | relu_3<br>ReLU | ReLU | 16×16×64 | - |
| 12 | conv_4<br>64 2×2×64 convolutions with stride [1 1] and padding 'same' | Convolution | 16×16×64 | Weights 2×2×64×64<br>Bias 1×1×64 |
| 13 | batchnorm_4<br>Batch normalization with 64 channels | Batch Normalization | 16×16×64 | Offset 1×1×64<br>Scale 1×1×64 |
| 14 | relu_4<br>ReLU | ReLU | 16×16×64 | - |
| 15 | maxpool_2<br>2×2 max pooling with stride [2 2] and padding [0 0 0 0] | Max Pooling | 8×8×64 | - |
| 16 | conv_5<br>128 2×2×64 convolutions with stride [1 1] and padding 'same' | Convolution | 8×8×128 | Weights 2×2×64×128<br>Bias 1×1×128 |
| 17 | batchnorm_5<br>Batch normalization with 128 channels | Batch Normalization | 8×8×128 | Offset 1×1×128<br>Scale 1×1×128 |
| 18 | relu_5<br>ReLU | ReLU | 8×8×128 | - |
| 19 | conv_6<br>128 2×2×128 convolutions with stride [1 1] and padding 'same' | Convolution | 8×8×128 | Weights 2×2×128×128<br>Bias 1×1×128 |

**Figure 4.18:** Proposed Method Layers.

# 5. CONCLUSION

## 5.1 CONCLUSION

A deep learning method was designed for the purpose of determining whether or not a fundus image was impacted by DR and whether or not it included hard exudates. In situations of diabetic retinopathy disease, it is essential to distinguish hard exudates so that the existence of illness may be automatically diagnosed. This is done so that treatment can begin sooner. The new method has a degree of confidence of 99.7 percent and can determine with pinpoint accuracy whether or not hard exudates are present. In the future, it will also be necessary to identify soft exudates, haemorrhage, and microaneurysms. In addition to this, we are going to use the segmented photos in order to measure the degree of DR. To improve the accuracy of the model, two different approaches have been suggested. The first thing you may do is play about with the dimensions of the photo patch. In the event that this takes place, we may look at how the image patches affect the accuracy of the forecast. The second method employs a collection of convolutional neural networks to conduct an analysis of the 16 unpredicted pixels located at the beginning and end of each row and column.

## 5.2 FUTURE WORK

Before we can make a forecast, we need to fix the picture by padding it with zeros so that we can tackle this problem. Our efforts are not sufficient enough to identify the hard exudates that have been produced. While producing patches, the first 16 pixels of each input picture are disregarded since padding is not utilized in the process. As a result of this, it is not possible for it to search for hard exudates at this point in time. This is a disadvantage due to the fact that evaluating the boundary pixels increases the likelihood of finding the hard exudates, which increases the importance of this step.

Another obstacle was the amount of time required training the neural network. The sheer magnitude of the image dataset was a significant contributor to this result. Because of this, we only used a portion of the whole dataset as our source of information.

# REFERENCES


[1] Chen, Wanghu, et al. "An approach to detecting diabetic retinopathy based on integrated shallow convolutional neural networks." IEEE Access 8 (2020): 178552-178562.

[2] World Health Organization and International Diabetes Federation (2005) Definition and diagnosis of diabetes mellitus and inter¬mediate hyperglycemia, a report of world health organization and international diabetes federation.

[3] International diabetes federation (2013) Diabetes atlas, 6th edn. Brussels, Belgium https://www.idf.org/sites/default/files/EN_6E_ Atlas_Full_0.pdf. Accessed 23 Jan 2018

[4] Veresiu AI, Bondor CI, Florea B, Vinik EJ, Vinik AI, Grivan NA (2015) Detection of undisclosed neuropathy and assessment of its impact on quality of life: a survey in 25,000 Romanian patients with diabetes. J Diabetes Complications 29(5):644—649

[5] Antal B, Hajdu A (2012) An ensemble-based system for microaneurysm detection and diabetic retinopathy grading. IEEE Trans Biomed Eng 59(6):1720

[6] Islam M, Dinh AV, Wahid KA (2017) Automated diabetic retinopathy detection using bag of words approach. J Biomed Sci Eng 10:86-96

[7] F. Al-Maskari and M. El-Sadig, “Prevalence of diabetic retinopathy in the United Arab Emirates: a cross-sectional survey,” BMC Ophthalmology, vol. 7, no. 1, pp. 1–8, 2007.

[8] Pathak, Ketki C., et al. "Diabetic Retinopathy Diagnosis and Categorization using Deep Learning-A Review." 2021 5th International Conference on Intelligent Computing and Control Systems (ICICCS). IEEE, 2021.

[9] Sisodia, Dilip Singh, Shruti Nair, and Pooja Khobragade. "Diabetic retinal fundus images: Preprocessing and feature extraction for early detection of diabetic retinopathy." Biomedical and Pharmacology Journal 10.2 (2017): 615-626.

[10] Goel, Silky, et al. "Deep Learning Approach for Stages of Severity Classification in Diabetic Retinopathy Using Color Fundus Retinal Images." Mathematical Problems in Engineering 2021 (2021).

[11] Miao, Yue, and Siyuan Tang. "Classification of Diabetic Retinopathy Based on Multiscale Hybrid Attention Mechanism and Residual Algorithm." Wireless Communications and Mobile Computing 2022 (2022).

[12] Das, Sraddha, et al. "Deep learning architecture based on segmented fundus image features for classification of diabetic retinopathy." Biomedical Signal Processing and Control 68 (2021): 102600.

[13] Zheng Y, Ley SH, Hu FB. Global aetiology and epidemiology of type 2 diabetes mellitus and its complications. Nat Rev Endocrinol. 2018 Feb;14(2):88-98.

[14] Riaz, Samreen. "Diabetes mellitus Sci Res Essay 2009 4367373. 2." Riaz S: Diabetes mellitus. Sci Res Essay 4 (2009): 367-373.

[15] Daly, B. et al. Increased risk of ischemic heart disease, hypertension, and type 2 diabetes in women with previous gestational diabetes mellitus, a target group in general practice for preventive interventions: a population-based cohort study. PLOS Med. 15, e1002488 (2018).

[16] Malek R, Hannat S, Nechadi A, Mekideche FZ, Kaabeche M. Diabetes and Ramadan: A multicenter study in Algerian population. Diabetes Res Clin Pract. 2019 Apr;150:322-330. [Abstract]

[17] Choi YJ, Chung YS. Type 2 diabetes mellitus and bone fragility: Special focus on bone imaging. Osteoporos Sarcopenia. 2016 Mar;2(1):20-24. [Abstract]

[18] Picke AK, Campbell G, Napoli N, Hofbauer LC, Rauner M. Update on the impact of type 2 diabetes mellitus on bone metabolism and material properties. Endocr Connect. 2019 Mar 01;8(3):R55-R70. [Abstract]

[19] Carrillo-Larco RM, Barengo NC, Albitres-Flores L, Bernabe-Ortiz A. The risk of mortality among people with type 2 diabetes in Latin America: A systematic review and meta-analysis of population-based cohort studies. Diabetes Metab Res Rev. 2019 May;35(4):e3139. [Abstract]

[20] Goyal, Rajeev, and Ishwarlal Jialal. "Diabetes mellitus type 2." (2018).

[21] McIntyre, H. David, et al. "Gestational diabetes mellitus." Nature reviews Disease primers 5.1 (2019): 1-19.

[22] Teo, Zhen Ling, et al. "Global prevalence of diabetic retinopathy and projection of burden through 2045: systematic review and meta-analysis." Ophthalmology 128.11 (2021): 1580-1591.

[23] Lee R, Wong TY, Sabanayagam C. Epidemiology of diabetic retinopathy, diabetic macular edema and related vision loss. Eye Vis [Internet] London BioMed Central. 2015;2:17.

[24] Yau JWY, Rogers SL, Kawasaki R, Lamoureux EL, Kowalski JW, Bek T, et al. Global prevalence and major risk factors of diabetic retinopathy. Diabetes Care [Internet]. Am Diabetes Assoc. 2012;35(3):556–64.

[25] Aiello LP, Gardner TW, King GL, Blankenship G, Cavallerano JD, Ferris FL, et al. Diabetic retinopathy. Diabetes Care [Internet]. 1998;21(1):143 LP–156.

[26] Pathak, Ketki C., et al. "Diabetic Retinopathy Diagnosis and Categorization using Deep Learning-A Review." 2021 5th International Conference on Intelligent Computing and Control Systems (ICICCS). IEEE, 2021.

[27] Robinson R, Barathi VA, Chaurasia SS, Wong TY, Kern TS. Update on animal models of diabetic retinopathy: from molecular approaches to mice and higher mammals. Dis Model Mech [Internet] Company Biologists Limited. 2012;5(4):444–56.

[28] C.A. Harper, J.E. Keeffe Diabetic retinopathy management guidelines Expet Rev Ophthalmol, 7 (5) (2012), pp. 417-439

[29] P.H. Scanlon, C.P. Wilkinson, S.J. Aldington, D.R. Matthews A Practical manual of diabetic retinopathy management (first ed.), Wiley-Blackwell (2009).

[30] Dubow, Michael, et al. "Classification of human retinal microaneurysms using adaptive optics scanning light ophthalmoscope fluorescein angiography." Investigative ophthalmology & visual science 55.3 (2014): 1299-1309.

[31] Bandello, Francesco, et al., eds. Clinical Strategies in the Management of Diabetic Retinopathy: A step-by-step Guide for Ophthalmologists. Berlin, Germany: Springer, 2014.

[32] Pathak, Ketki C., et al. "Diabetic Retinopathy Diagnosis and Categorization using Deep Learning-A Review." 2021 5th International Conference on Intelligent Computing and Control Systems (ICICCS). IEEE, 2021.

[33] B. Zhou, X. Ai, and J. Fang, "Data-adaptive robust unit commitment in the hybrid AC/DC power system," *Applied Energy*, vol. 254, no. 15, pp. 1–12, 2019.

[34] S. Li, L. Liu, and A. Yan, "A compact field-portable double-pulse laser system to enhance laser induced breakdown spectroscopy," *Review of Scientific Instruments*, vol. 88, no. 2, pp. 23109–23115, 2017.

[35] B. Aifaa and B. Pal, "Adaptive protection and control in power system for wide-area blackout prevention," IEEE Transactions on Power Delivery, vol. 4, no. 2, pp. 1815–1825, 2016.

[36] Chen, Chaofan, et al. "This looks like that: deep learning for interpretable image recognition." Advances in neural information processing systems 32 (2019).

[37] Hashimoto DA, Rosman G, Rus D, Meireles OR. Artificial intelligence in surgery: promises and perils. Ann Surg 2018;268:706.

[38] Ahmad, M. Sheraz, et al. "An efficient heart murmur recognition and cardiovascular disorders classification system." Australasian physical & engineering sciences in medicine 42.3 (2019): 733-743

[39] Tsiknakis, Nikos, et al. "Deep learning for diabetic retinopathy detection and classification based on fundus images: A review." Computers in Biology and Medicine 135 (2021): 104599

[40] Miller DD, Brown EW. Artificial intelligence in medical practice: the question to the answer? Am J Med 2018;131(2):12933.

[41] Kirch DG, Petelle K. Addressing the physician shortage: the peril of ignoring demography. JAMA 2017;317(19):19478.

[42] Bresnick J. Artificial intelligence in healthcare market to see 40% CAGR surge; 2017.

[43] Marr B. How is AI used in healthcare—5 powerful real-world examples that show the latest advances. Forbes; 2018.

[44] Nahid A, Mikaelian A, Kong Y (2018) Histopathological breast-image classification with restricted Boltzmann machine along with backpropagation. Biomed Res 29(10)

[45] Dutta S, Manideep BC, Basha SM, Caytiles RD, Iyengar NCSN (2018) Classification of diabetic retinopathy images by using deep learning models. Int J Grid Distrib Comput 11(1):99–106

[46] Das, Sraddha, et al. "Deep learning architecture based on segmented fundus image features for classification of diabetic retinopathy." Biomedical Signal Processing and Control 68 (2021): 102600.]

[47] Prasad DK, Vibha L, Venugopal K (2015) Early detection of diabetic retinopathy from digital retinal fundus images. 2015 IEEE Recent Advances in Intelligent Computational Systems (RAICS)]

[48] Alzami, Farrikh, Rama Arya Megantara, and Ahmad Zainul Fanani. "Diabetic retinopathy grade classification based on fractal analysis and random forest." 2019 International Seminar on Application for Technology of Information and Communication (iSemantic). IEEE, 2019.

[49] Qomariah, Dinial Utami Nurul, Handayani Tjandrasa, and Chastine Fatichah. "Classification of diabetic retinopathy and normal retinal images using CNN and SVM." 2019 12th International Conference on Information & Communication Technology and System (ICTS). IEEE, 2019.

[50] Kumar, Shailesh, and Basant Kumar. "Diabetic retinopathy detection by extracting area and number of microaneurysm from colour fundus image." 2018 5th International Conference on Signal Processing and Integrated Networks (SPIN). IEEE, 2018.

[51] T. Shanthi and R. S. Sabeenian, "Modified Alexnet architecture for classification of diabetic retinopathy images," Computers & Electrical Engineering, vol. 76, pp. 56–64, 2019.

[52] K. O'Shea and R. Nash, "An introduction to convolutional neural networks," arXiv preprint arXiv:1511.08458, 2015.

[53] G. Litjens et al., "A survey on deep learning in medical image analysis," Medical image analysis, vol. 42, pp. 60–88, 2017.

[54] M. Shaban, A. H. Mahmoud, A. Shalaby, M. Ghazal, H. Sandhu, and A. El-Baz, "Low-complexity computer-aided diagnosis for diabetic retinopathy," Diabetes and retinopathy, pp. 133–149, 2020.

[55] H. Pratt, *Deep Learning for Diabetic Retinopathy Diagnosis & Analysis*. The University of Liverpool (United Kingdom), 2019.

[56] D. Cornelisse, "An intuitive guide to convolutional neural networks," *free Code Camp*, pp. 1–19, 2018.

[57] S.Kannoju, "DIABETIC RETINOPATHY DETECTION USING RETINAL IMAGES," Sacramento, 2021.

[58] E. Abdelmaksoud, S. El-Sappagh, S. Barakat, T. Abuhmed, and M. Elmogy, "Automatic diabetic retinopathy grading system based on detecting multiple retinal lesions," *IEEE Access*, vol. 9, pp. 15939–15960, 2021.

[59] S. Ruder, “An overview of gradient descent optimization algorithms,” *arXiv preprint arXiv:1609.04747,* 2016.

[60] D. P. Kingma and J. Ba, “Adam: A method for stochastic optimization,” *arXiv preprint arXiv:1412.6980,* 2014.

[61] A. Krogh and J. Vedelsby, “Neural network ensembles, cross validation, and active learning,” *Advances in neural information processing systems*, vol. 7, 1994.

[62] I. Arias-Serrano et al., “Artificial intelligence based glaucoma and diabetic retinopathy detection using MATLAB — retrained AlexNet convolutional neural network,” F1000Research 2023 12:14, vol. 12, p. 14, Jan. 2023, doi: 10.12688/f1000research.122288.1.

[63] M. M. Abdelsalam, “Effective blood vessels reconstruction methodology for early detection and classification of diabetic retinopathy using OCTA images by artificial neural network,” Inform Med Unlocked, vol. 20, p. 100390, Jan. 2020, doi: 10.1016/J.IMU.2020.100390.

[64] X. Li, T. Pang, B. Xiong, W. Liu, P. Liang, and T. Wang, “Convolutional neural networks based transfer learning for diabetic retinopathy fundus image classification,” Proceedings - 2017 10th International Congress on Image and Signal Processing, BioMedical Engineering and Informatics, CISP-BMEI 2017, vol. 2018-January, pp. 1–11, Feb. 2018, doi: 10.1109/CISP-BMEI.2017.8301998.

[65] D. J. Hemanth, O. Deperlioglu, and U. Kose, “An enhanced diabetic retinopathy detection and classification approach using deep convolutional neural network,” Neural Comput Appl, vol. 32, no. 3, pp. 707–721, Feb. 2020, doi: 10.1007/S00521-018-03974-0/FIGURES/10.

[66] A. K. Al-Bashir and A. N. A. Obeid, “Automatic Discrimination between Normal and Diabetic Retinopathy Fundus Images using Machine Learning Classification Algorithm,” Proceedings - 2022 International Conference on Image Processing and Media Computing, ICIPMC 2022, pp. 35–40, 2022, doi: 10.1109/ICIPMC55686.2022.00015.

[67] Z. Ying, “Classification of Diabetic Retinopathy Based on B-ResNet,” Proceedings - 2022 7th IEEE International Conference on Data Science in Cyberspace, DSC 2022, pp. 570–575, 2022, doi: 10.1109/DSC55868.2022.00085.